From random to rational: A discovery approach to selective subnanomolar inhibitors of human carbonic anhydrase IV based on

From Random to Rational: A Discovery Approach to Selective Subnanomolar Inhibitors of Human Carbonic Anhydrase IV Based on the Castagnoli-Cushman Multicomponent Reaction

Stanislav Kalinin[a], Alessio Nocentini[b], Alexander Kovalenko[a], Vladimir Sharoyko[a], Alessandro Bonardi[b], Andrea Angeli[b], Paola Gratteri[b], Tatiana B. Tennikova[a], Claudiu T. Supuran[b,x] Mikhail Krasavin[a,x]

[a] Saint Petersburg State University, Saint Petersburg, 199034 Russian Federation

[b] Neurofarba Department, Universita degli Studi di Firenze, Florence, Italy

xCorresponding authors. E-mail addresses: m.krasavin@spbu.ru (M. Krasavin), claudiu.supuran@unifi.it (C. T. Supuran)

ABSTRACT

By exploiting the power of multicomponent chemistry, a relatively small, diverse set of primary sulfonamides was synthesized and screened against a panel of human carbonic anhydrases to reveal a low-nanomolar, albeit non-selective *h*CA IV lead inhibitor. Investigation of the docking poses of this compound identified a hydrophilic pocket unique to *h*CA IV and conveniently positioned near the carboxylate functionality of the initial lead. Various residues capable of forming hydrogen bonds as well as salt bridges were placed in this pocket via a carboxamides linkage, which led to drastic improvement of potency and selectivity towards *h*CA IV. This improvement of the desired inhibitory profile was rationalized by the new contacts as had been envisioned. These new tool compounds were shown to possess selective, dose-dependent cytotoxicity against human glioma T98G cell line. The latter showed a substantially increased *h*CA IV mRNA expression under hypoxic conditions.

Keywords: carbonic anhydrase; isoform-selective inhibitors; scaffold; periphery groups; Castagnoli-Cushman reaction; seed SAR; primary sulfonamides; *in silico* docking; subnanomolar inhibition; cancer cells; hypoxic environment.

1. Introduction

Reversible hydration of carbon dioxide producing bicarbonate anion and a proton is a fundamental biochemical reaction responsible for controlling intra- and extracellular pH. Numerous physiological processes depend on this simple reaction catalyzed by the human carbonic anhydrases (*h*CAs) [1]. The 15 *h*CA isoforms have different cellular localization,

catalytic activity and expression levels in normal *vs.* aberrantly functioning cells [2]. Some of these isoforms are already validated targets for drug intervention in various disease states. Yet, novel links to pathological disorders continue to be discovered [3].

Today, however, all clinically used carbonic anhydrase inhibitors (such as diuretics [4] or drugs used to treat glaucoma-related intraocular hypertension [5]) are predominantly non-selective with respect to *h*CA isoforms (Fig. 1). Apparently, the potent, albeit non-selective inhibition of *h*CA II (the primary target [6]) exerted by these drugs is sufficient for attaining therapeutic effect in these diseases. However, development of novel therapeutic agents based on *h*CA inhibition or continued validation of specific *h*CA isoforms as drug targets requires that selective inhibitors for the isoform in question are developed. Not only is selectivity desirable for reducing off-target *h*CA inhibition (and, hence, the drug side effects), the absence of selective inhibitor tool compounds retards the establishment of the links between aberrant hyperactivity of certain *h*CA isoforms in search for emerging therapeutic options [7].

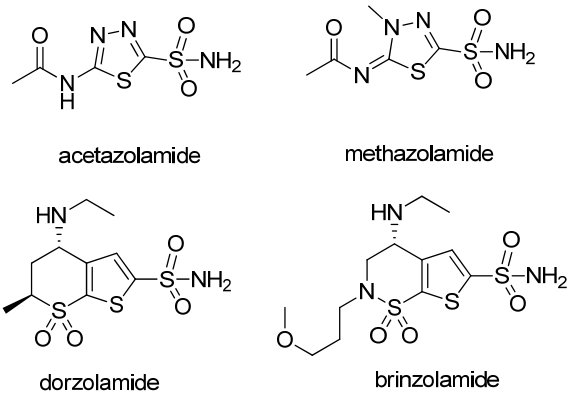

Fig. 1. Examples of clinically used, non-selective *h*CA inhibitors.

The landscape of investigational isoform-selective carbonic anhydrase inhibitors (CAIs) has been steadily widening. Examples worth noting include isoxazole bis-sulfonamide inhibitor of membrane-bound *h*CA IV (**1**) [8], dual inhibitor of cytosolic *h*CA II and VII based on 2-imidazoline scaffold (**2**) [9], selective biphenyl sulfonamide inhibitor of *h*CA XIV (**3**) [10], and ring-opened *N*-alkyl saccharin derivative (**4**) selective for tumor-associated, membrane-bound isoforms *h*CA IX and XII [11]. In the clinical phases of development, *h*CA IX-selective drug SLC-0111 has now successfully completed phase I clinical trials for tumors overexpressing CA IX [12] and is scheduled [13] to enter phase II clinical trials in the near future (Figure 2).

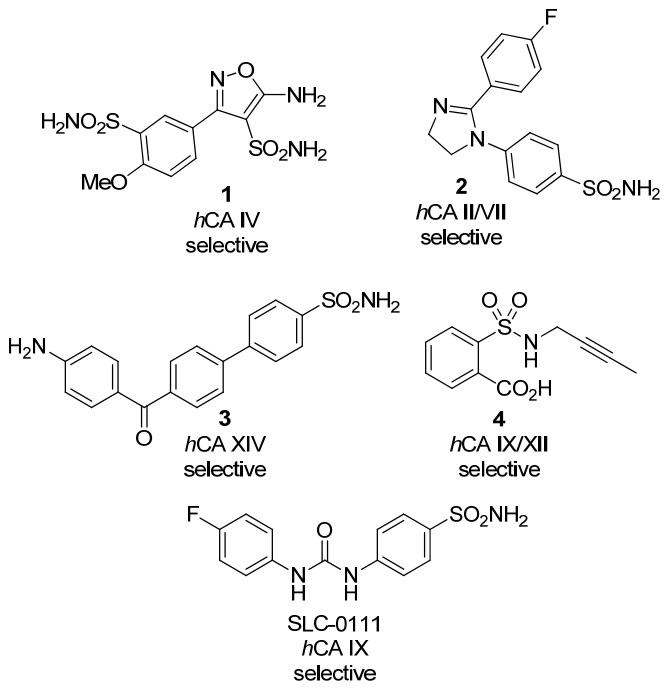

Fig. 2. Examples of recently reported isoform-selective *h*CA inhibitors (**1**-**4**) and the structure of the most advanced *h*CA IX-selective CAI (SLC-0111) currently in clinical trials for cancer.

From the current literature, it can be concluded that some *h*CA isoforms are more challenging to target selectively compared to others. An example of such a difficult-to-target isoform is *h*CA IV – a membrane-bound enzyme with medium catalytic activity and high affinity to primary sulfonamides, the most prominent class of carbonic anhydrase inhibitors acting *via* binding to the prosthetic Zn^{2+} ion in the active site [14]. It is expressed in the kidney, lung, pancreas, brain capillaries, colon, heart muscle, eye [15] and, most importantly, on the surface of astrocytes [16], the characteristic star-shaped glial cells in the brain and spinal cord accounting for 20% to 40% of all glia [17]. It is *h*CA IV on the membrane of astrocytes that is responsible for regulating interstitial pH [16] and for regulating transmembrane lactate transport [18-19] (although it has also been proposed that the latter could be regulated by non-catalytic action of *h*CA II [20]). More recently, the involvement of *h*CA IV in the lactate transport has been speculated to occur *via* interaction with monocarboxylate transporter's chaperones [21]. Currently, targeting of *h*CA IV with inhibitors doesn't have clear therapeutic applications [22]. However, the isoform was shown to be involved in such diseases as retinitis pigmentosa and glaucoma [23] and its involvement in the pH regulation makes it probable that its inhibition can be beneficial approach to treat astrocytomas and gliomas in general, similarly to inhibition of other membrane-bound isoforms *h*CA IX and XII which is a validated approach to cancer treatment awaiting clinical proof-of-concept [24].

Taking this notion to the stage of validated concept for therapeutic intervention, however, would require that selective *h*CA IV inhibitors are in place. These, however, are not easy to come by.

Besides compound **1** (Figure 2), only a limited number of compounds with pronounced inhibitory selectivity and/or potency toward hCA IV have been reported to-date [25-28]

The goal of designing isoform-specific carbonic anhydrase inhibitors (CAIs) is particularly difficult in light of significant similarity of amino acid composition and active site architecture of *h*CA isoforms [29]. Thus, docking into a particular isoform crystal structure, while certainly capable of providing clues as to the potential of a given chemotype to inhibit *h*CA in general, has not been sufficient to predict the absence of strong inhibition of off-target isoforms. In fact, biochemical profiling of such *in silico* prioritized compounds against a panel of *h*CAs, has been a rich source of serendipitously discovered inhibitors of various isoforms besides those whose crystal structures were initially used for docking. This is illustrated by the selected recent examples from the literature shown in Table 1.

Table 1. Examples of target-based design of CAIs illustrating limitations of *in silico* docking in predicting isoform specificity.

Entry	*h*CA crystal structure used for docking (PDB code)	Additional *h*CA isoforms inhibited	Reference
1	*h*CA II (PDB 4Z0Q)	*h*CA VII	[30]
2	*h*CA II (PDB 1CA2)	*h*CA VII, IX and other	[31, 32]
3	*h*CA IX (*h*CA XIV-based homology model, PDB 1RJ5)	*h*CA I, II	[33, 34]
4	*h*CA II (PDB 3B4F)	*h*CA I, VII, XIV	[35]
5	*h*CA IX (PDB 3IAI)	*h*CA II	[36]

Although efforts are underway to rationally exploit differences in the surface amino acid composition of different *h*CA isoforms (i. e. outside of the enzyme's active site) [37], most of the currently discovered isoform-specific *h*CA inhibitors originate from screening of chemically diverse libraries of primary sulfonamides against a panel of *h*CAs [38-41]. Considering that such a serendipity-based approach requires sufficiently large chemical space is investigated. Despite the recent efforts aimed at developing high-throughput carbonic anhydrase assays [42-43], the medium-throughput stopped-flow CO_2 hydratase assay [44] remains the golden standard assay for this class of enzymes. Therefore, the compound libraries intended for screening should be as chemically diverse as possible.

Multicomponent reactions are undoubtedly the most powerful tool for library synthesis offering a diligent, informative, SAR-tractable sampling of the chemical space with maximum achievable

diversity of the compounds' periphery appendages [45]. However, multicomponent chemistry remains rather poorly exploited in the design of carbonic anhydrase inhibitors [46]. We have been recently engaged in developing novel scaffold-oriented syntheses based on the powerful cycloaddition reaction between α-C-H dicarboxylic acid anhydrides and imines (prepared in a separate step or generated in situ from primary amines and aldehydes or ketone) known as the Castagnoli-Cushman reaction (CCR) [47]. The reaction allows simultaneously varying the scaffold and the periphery elements which is a rather unique feature among multicomponent reactions at large. It is exploiting this feature that facilitated the recent discovery of new CCR-derived antagonists of the oncogenic MDM2-p53 protein-protein interaction [48]. In this work, we decided to apply the CCR as a chemical space-sampling tool toward creating a scaffold- and periphery-diverse set of sulfonamides of type A and B having the sulfonamide group either in the amine- or the aldehyde-derived portion of the lactams molecule, respectively (Figure 3). We reasoned that the densely functionalized Castagnoli-Cushman lactams may not only deliver a promising initial 'seed SAR' information but will allow for a rational, structure-based optimization of the first-iteration leads. Herein, we present the results obtained in reducing this approach to practice.

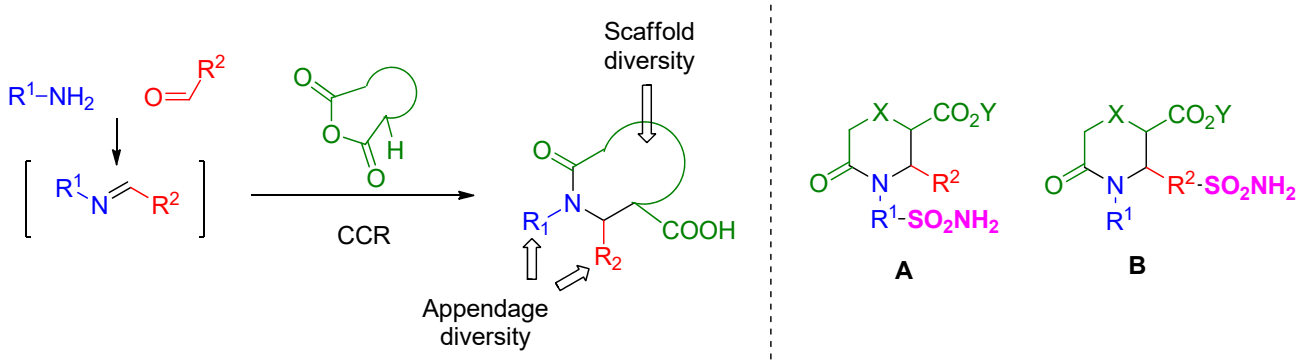

Figure 3. The Castagnoli-Cushman reaction (CCR) and the CCR-derived primary sulfonamides investigated in this work.

2. Results and discussion

2.1. Synthesis of the first-iteration ('seed SAR') sulfonamides

The initial experimentation aimed at involving sulfonamide-functionalized imines **5a-b** in the CCR with a range of cyclic anhydrides (including the ones successfully employed in an alternative approach described below) revealed that these imines (**5a-b**) are completely unreactive, neither in the free or the protected form. This is likely due to the high electron-withdrawing character of the 4-sulfamoyl phenyl group which deactivated the imine nitrogen atom toward acylation by the anhydride regardless of its position relative to the imine C=N bond

[49-50]. Hence, we needed to introduce the required primary sulfonamide functionality in a later stage while using building blocks containing a 'masked sulfonamide' functionality for the CCR. Such an approach was realized with benzenethio-substituted imines **6a-g** and **6h-m** (prepared in a separate step from 4-(benzylthio)benzaldehyde and 4-(benzylthio)aniline, respectively). Using the recently developed solvent-free protocol for the CRR [50], the imines **6a-m** were involved in the cyclocondensation with succinic (**7a**), diglycolic (**7b**) and mesyl-protected iminodiacetic (**7c**) anhydrides to give predominantly *trans*-configured [49] CCR lactams converted to methyl esters **8a-h** and **9a-h** (for easier purification) in moderate yields over two steps. Subsequent unmasking of the primary sulfonamide function was achieved in a two-step protocol involving *N*-chloroduccinimide (NCS) oxidation and treatment of the intermediate sulfochloride with aqueous ammonia [51]. This furnished the desired sulfonamides **10a-h** and **11a-h** in good yields over two steps and was not accompanied by the loss of the relative stereochemical integrity, according to the characteristic methine proton splitting pattern in the ^{1}H NMR spectra [49] (Scheme 1).

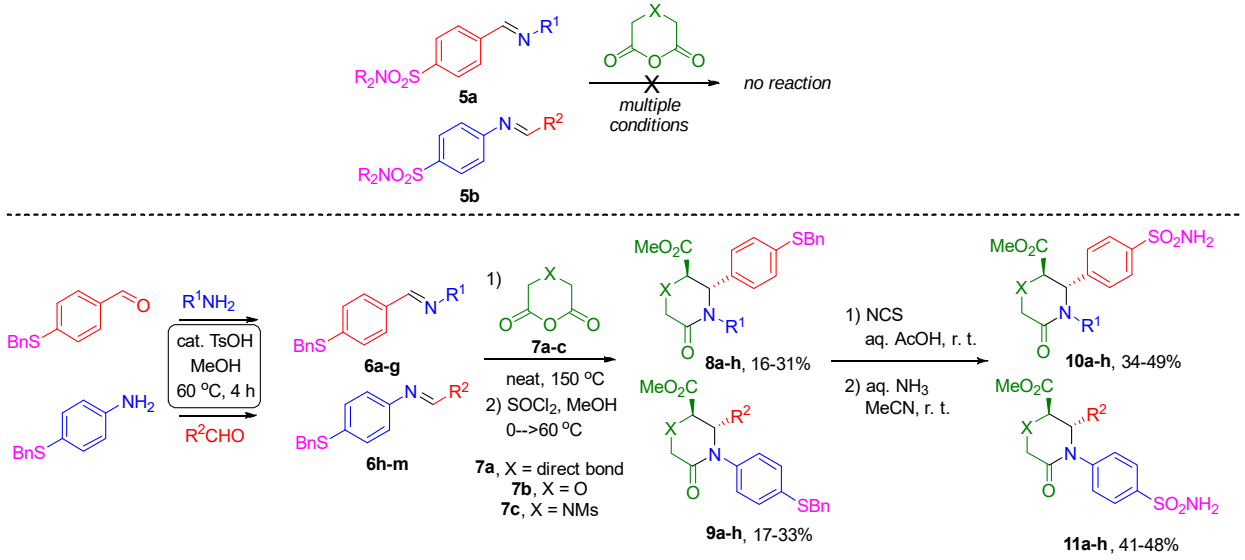

Scheme 1. Failed and successfully realized syntheses of the sulfonamide lactams **10(11)a-h** *via* the CCR.

2.2 Inhibitory profile of the initial, 'seed SAR' set against a panel of hCAs

The 16 primary sulfonamide lactams **10a-h** and **11a-h** synthesized as detailed above, were tested in CO_2 hydration stopped-flow biochemical assay (see Experimental section) [44] against hCA I, II, IV and VII isoforms to produce the inhibition data (K_i) summarized in Table 1.

Considering that this set of compounds had been designed to probe isoform selectivity by establishing the 'seed SAR' (i. e. the initial potency and selectivity trends that could be later used to develop selective tool inhibitors, particularly of *h*CA IV isoform), we analyzed these data from that angle. The entire subset of eight compounds **10a-h** having the sulfonamide

pharmacophore in the 'aldehyde' portion of the CCR-derived lactam scaffold, showed neither a promising potency nor selectivity toward hCA IV. There is a clear tendency in that subset to inhibit *h*CA II (well established target for glaucoma drugs and diuretics [6]) and *h*CA VII (a target for neuropathic pain [38]). While inhibition of the latter isoform displayed fairly 'flat' SAR with K_i values in the double-digit nanomolar range, the former was inhibited occasionally in the low nanomolar range (**10c**, **10f**). A notable profile was displayed by the only morpholinone compound tested (**10h**) which showed a remarkable selectivity toward *h*CA VII and will be subject of a separate study.

The other subset of the 'seed SAR group of compounds (**11a-h**) had the pharmacophore sulfonamide moiety in the 'amine' portion of the CCR-derived lactam scaffold. Generally, it had a greater overall potency toward *h*CA at large. However, it was the low nanomolar inhibition of *h*CA IV by compound **11d** that caught our attention. While being virtually non-selective *vs.* the other three isoforms, this chemotype in general displayed fairly sensitive SAR (*cf.* **11d**, **11b**, **11e** – all based on the same pyrrolidin-2-one scaffold). Considering that potent inhibitors of this isoform are exceedingly rare [28] and selective ones are even scarcer (*vide supra*) we considered **11d** a promising lead identified by the 'seed SAR' approach which could be subsequently rationally developed into a selective *h*CA IV inhibitor with the aid of target-based design.

Table 1. Inhibitory profile of compounds **7a-e** and **8a-s** against *h*CA I, II, IV and VII.[a]

Compound	X	R^1	R^2	K_i (nM)			
				*h*CA I	*h*CA II	*h*CA IV	*h*CA VII
10a	direct bond	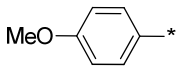	-	441.4	18.4	885.6	43.3
10b	direct bond	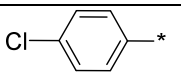	-	501.7	153.8	8695.3	28.6
10c	direct bond	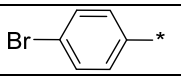	-	798.8	8.7	974.4	30.4
10d	direct bond	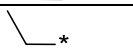	-	764.2	38.2	542.9	48.1
10e	direct bond	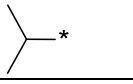	-	729.9	27.9	433.2	56.4
10f	NMs	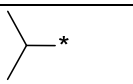	-	479.4	94.4	433.8	85.4
10g	NMs	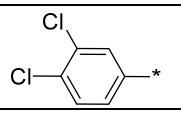	-	816.3	5.2	521.3	85.4
10h	O	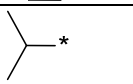	-	618.4	9103.9	9719.5	55.0
11a	direct bond	-	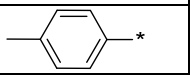	51.0	4.8	71.7	49.4

11b	direct bond	-	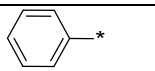	81.5	61.7	958.0	78.8
11c	direct bond	-	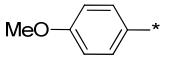	9.1	4.9	443.6	81.7
11d	direct bond	-	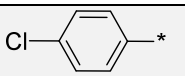	9.2	3.7	**9.6**	34.0
11e	direct bond	-	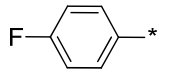	351.7	2.6	80.5	86.3
11f	NMs	-	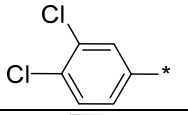	513.5	65.0	713.3	65.1
11g	NMs	-	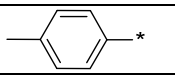	91.3	56.4	778.4	79.2
11h	O	-	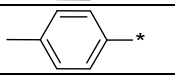	8.9	3.8	607.9	78.7
acetazolamide				250.0	12.1	74.0	6.0

[a] Mean from 3 different assays, by a stopped flow technique (errors were in the range of ± 5-10 % of the reported values).

*2.3 In silico docking of the lead (**11d**) to define ways to improve hCA IV selectivity*

With the potent (albeit non-selective) benchmark *h*CA IV inhibitor **11d** at hand, we proceeded to define its likely binding mode with the target as identify possible opportunities to increase the affinity of its congeners by building additional interactions with amino acid residues that are unique to *h*CA IV. Both enantiomers (*R,R*)-**11d** and (*S,S*)-**11d** were separately docked into the *h*CA IV crystal structure using the induced-fit docking procedure followed by refinement **with** the MM-GBSA (molecular mechanics/generalized Born surface area continuum solvation) method [52] (see Experimental Section). The minimum-energy docking poses thus obtained are shown in Figure 4.

For both enantiomers, the orientation of the benzenesulfonamide motif is the same as for the majority of such ligands in the *h*CA active site, providing anchoring to the prosthetic zinc metal ion [53]. Likewise, the pyrrolidin-2-one scaffold adopts a fully superimposable disposition in both enantiomers. The position of the 4-chlorophenyl fragment is distinctly different in the two enantiomers. In (*R,R*)-**11d**, this substituent points towards Thr202 and Asp204 forming weak H-bonds through the chlorine atom with the backbone NH of both residues and further VdW contacts with their side chains. Additionally, the benzene ring forms π-alkyl interactions with the Leu198 side chain. The methyl ester moiety did not appear to be involved in significant contacts with the binding site residues, though pointing towards the "right-hand side" (Figure 4A) of the hydrophilic/charged area of *h*CA IV active site. For (*S,S*)-**11d**, less favorable and more hindered binding was displayed by the 4-chlorophenyl portion. It accommodates at the edge between the lipophilic pocket line by Leu198, Ile141 and Val121, and the "middle" hydrophilic area of the binding site (Figure 4B). Such a positioning is likely driven by hydrophobic contacts of the aromatic portion with Leu198 and Ile141 side chains and VdW interactions with the Glu123

carboxylate moiety. Similarly to the other enantiomer (Figure 4C), the methyl ester group in (*S,S*)-**11d** points to the outer edge of the active site, towards the same hydrophilic area of the cavity (termed herein 'pocket A', *vide infra*).

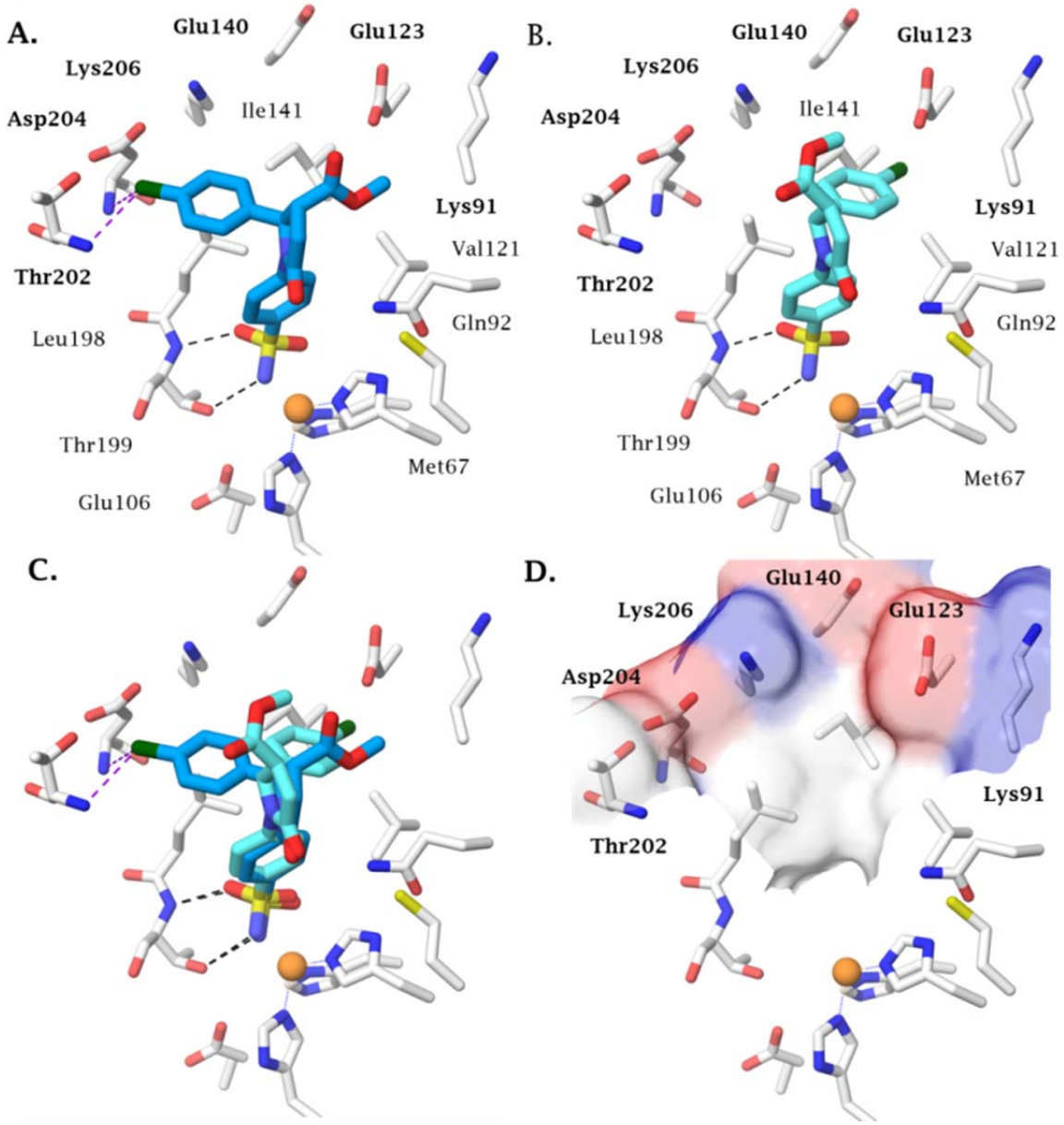

Figure 4. Predicted binding orientation of A) ***R,R*-11d**, B) ***S,S*-11d** and C) superposition of the both enantiomers in the *h*CA IV active site; D) surface representation of the *h*CA IV targeted (pocket A).

The principal unique structural feature of *h*CA IV which clearly distinguishes its binding site from those of other *h*CAs is the presence of a strongly hydrophilic/charged area ("pocket A" formed by Lys91, Glu132, Glu140, Lys206, Asp204 and Thr202 residues) which partially replaces the hydrophobic cleft typical of other α-CAs (Figure 1D). Considering that in both enantiomers of **11d**, this area is pointed to by the methoxycarbonyl group and this group is not involved in any principal contacts, we reasoned that the affinity towards *h*CA IV (and,

consequently, the selectivity) can be increased by attaching various hydrogen bond donor/acceptor (HBD/HBA) moieties as well as ionizable carboxylic acid groups (to explore potential salt bridge contacts with the lysine side chains) to the core of **11d** via a carboxamides linkage and, thereby, forming new contacts with the pocket A residues. Thus, the goal for the second stage of developing a potent and selective inhibitor of *h*CA IV isoform was to synthesize and investigate appropriately functionalized carboxamide analogs of **11d**.

2.4 Second iteration: attachment of carboxamides side chains

Compound **11d** was prepared of multigram scale and was hydrolyzed to carboxylic acid **12** with retention of relative stereochemistry. Acid **12** was activated with 1,1′-carbonyldiimidazole (CDI) and amidated with a range of amines bearing various HBA/HBD moieties to give amides **13a-r** in good isolated yields (see Experimental Section). Amides containing ester groups (**13i-l**) were subjected to alkaline hydrolysis to liberate hydroxylic groups (**13s-t**) or carboxylic acid functionalities (**13u-w**) in excellent yields (Scheme 2).

Scheme 2. Installment of HBD/HBD side chains in the second-iteration analogs of **11d**.

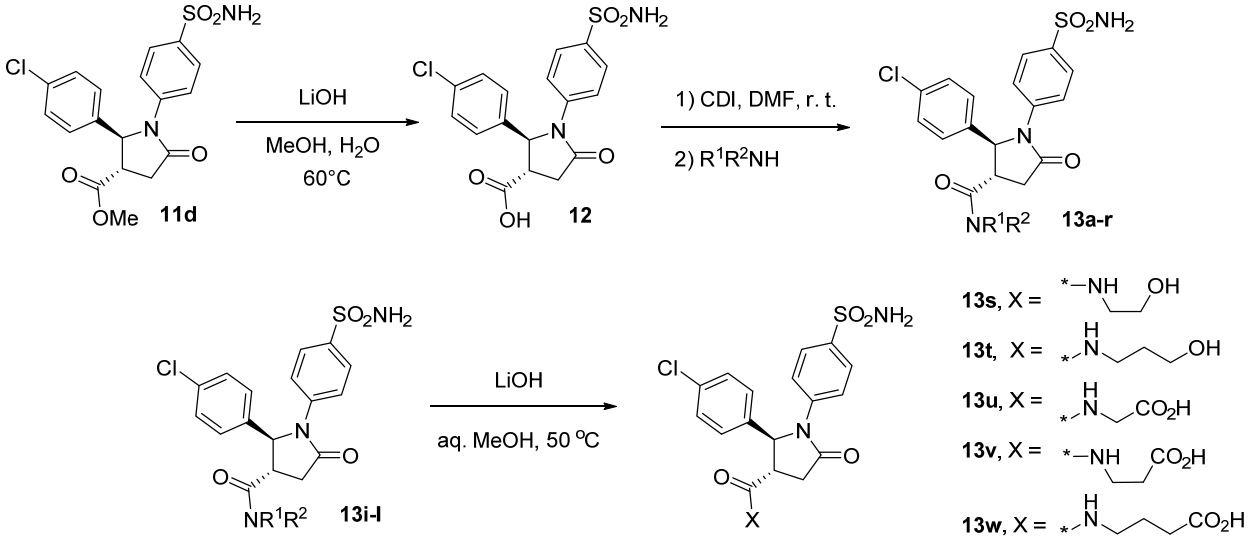

2.5 Inhibitory profile of the second-iteration CCR-derived lactams against hCAs.

Carboxylic acid **12** as well as twenty-three second-iteration carboxamides **13a-w** derived from it were tested in CO_2 hydration stopped-flow biochemical assay [44] against the same *h*CA isoforms as the first-iteration lead **11d** to produce the inhibition data (K_i) summarized in Table 2.

Table 2. Inhibitory profile of compounds **13a-w** against *h*CA I, II, IV and VII.[a]

Compound	NR^1R^2	K_i (nM)			
		*h*CA I	*h*CA II	*h*CA IV	*h*CA VII
12	-	350.4	44.8	25.1	48.3
13a	NH_2	941.1	57.3	68.7	69.0
13b	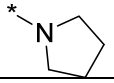	3 285	30.0	84.8	96.4

13c	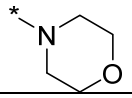	314.1	7.8	31.3	33.9
13d	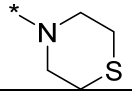	256.4	4.6	21.9	18.9
13e	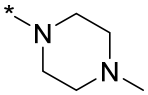	819.3	4.5	4.7	58.0
13f	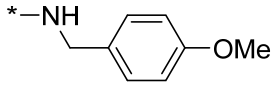	2 125	1.6	2.1	5.8
13g	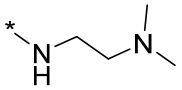	285.5	19.8	1.2	18.1
13h	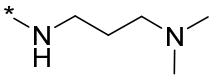	960.2	8.9	0.52	9.5
13i	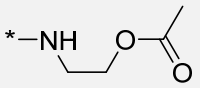	1 066	13.3	0.59	46.8
13j	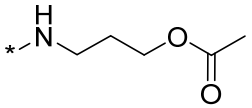	5 093	8.5	1.8	85.5
13k	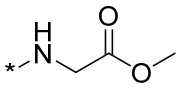	495.5	3.4	2.40	4.8
13l	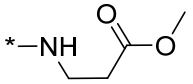	649.0	7.5	1.0	46.3
13m	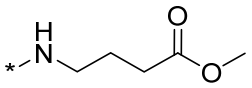	105.1	34.9	6.5	69.3
13n	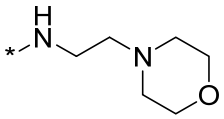	517.7	5.9	0.61	5.6
13o	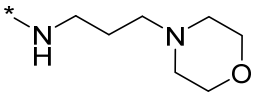	101.8	6.7	1.5	70.2
13p	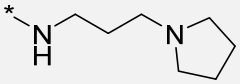	720.3	40.6	0.89	174.5
13q	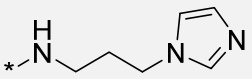	7 797	32.6	0.66	304.1
13r	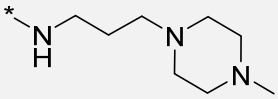	748.1	9.5	0.39	34.6
13s	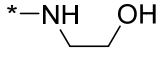	369.6	4.8	0.9	62.8
13t	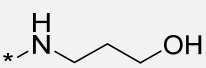	6 092	7.9	0.22	80.6

13u	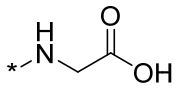	87.3	5.8	0.65	3.0
13v	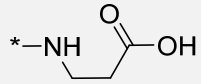	886.7	26.3	0.31	41.3
13w	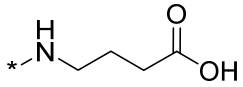	737.1	37.3	1.8	52.2
11d	-	9.2	3.7	9.6	34.0
acetazolamide		250.0	12.0	75.0	2.5

[a] Mean from 3 different assays, by a stopped flow technique (errors were in the range of ± 5-10 % of the reported values).

Examination of the data in Table 2 clearly reveals the positive outcome of the undertaken modification for improving the inhibitory potency and selectivity toward *h*CA IV isoform. The single-digit nanomolar inhibition of *h*CA I by **11d** was apparently weakened by 2-3 orders of magnitude throughout the second-generation analogs. At the same time, some analogs displayed one order of magnitude loss in potency against *h*CA II and VII (e. g., **13p-q**) while gaining potency by about the same factor against the target *h*CA IV isoform (**13i**, **13n**, **13p-v**). Clearly, the modification introduced in the second-iteration, aimed at building contacts with the HBA, HBD and positively changed side-chain residues in 'pocket A' which is unique to hCA IV, resulted in many subnanomolar inhibitors of that isoform, thereby attesting to the correctness of the design strategy. Among these subnanomolar *h*CA IV inhibitors, compounds **13i, 13p, 13q, 13r, 13t** and **13v** showed the best selectivity profiles as illustrated by their selectivity indices, SI(*h*CA Y) = K_i(*h*CAY)/K_i(*h*CAIV) shown in Figure 5.

Figure 5. Selectivity indices (SI) of compounds **13i, 13p, 13q, 13r, 13t** and **13v** against *h*CA I, II and VII relative to the target (*h*CA IV) isoform (in log units).

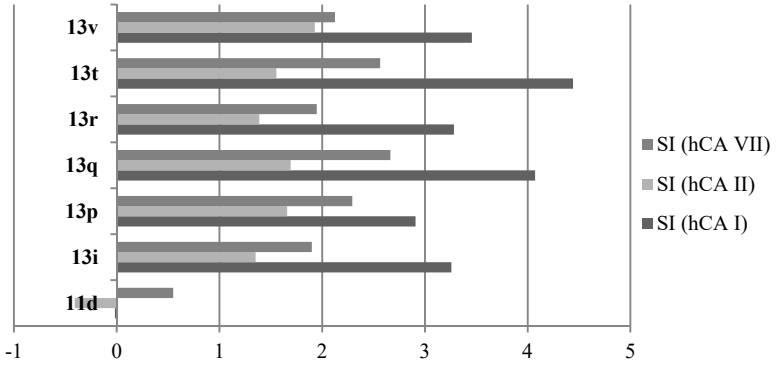

The best selectivity improvement in the second iteration was apparently achieved with compounds **13p-q** and **13v** having drastically different side chains. This, one hand, justified the correctness of unbiased "HBD/HBA" approach to targeting both types of interactions in "pocket A" as well potential electrostatic

(salt bridge) contact which is likely the case with carboxylic acid **13v**. On the other hand we became curious if these hypothetical binding modes can be visualized as the low-energy complex *via* docking.

2.6 Docking studies of the second-iteration selective nanomolar hCA IV inhibitors

Compounds **13p**, **13q** and **13v** turned out as the most selective for *h*CA IV over the ubiquitous *h*CA I and II as well as *h*CA VII and were subject to *in silico* studies to show the interactions driving their subnanomolar inhibition efficacy for the target (*h*CA IV) isoform. Induced-fit docking procedures were used to allow the movement of the active site residues, particularly those of pocket A that are more exposed to the solvent. Both enantiomers of the three compounds were evaluated. MM-GBSA-based refinements led to the binding predictions reported in Figure 5.

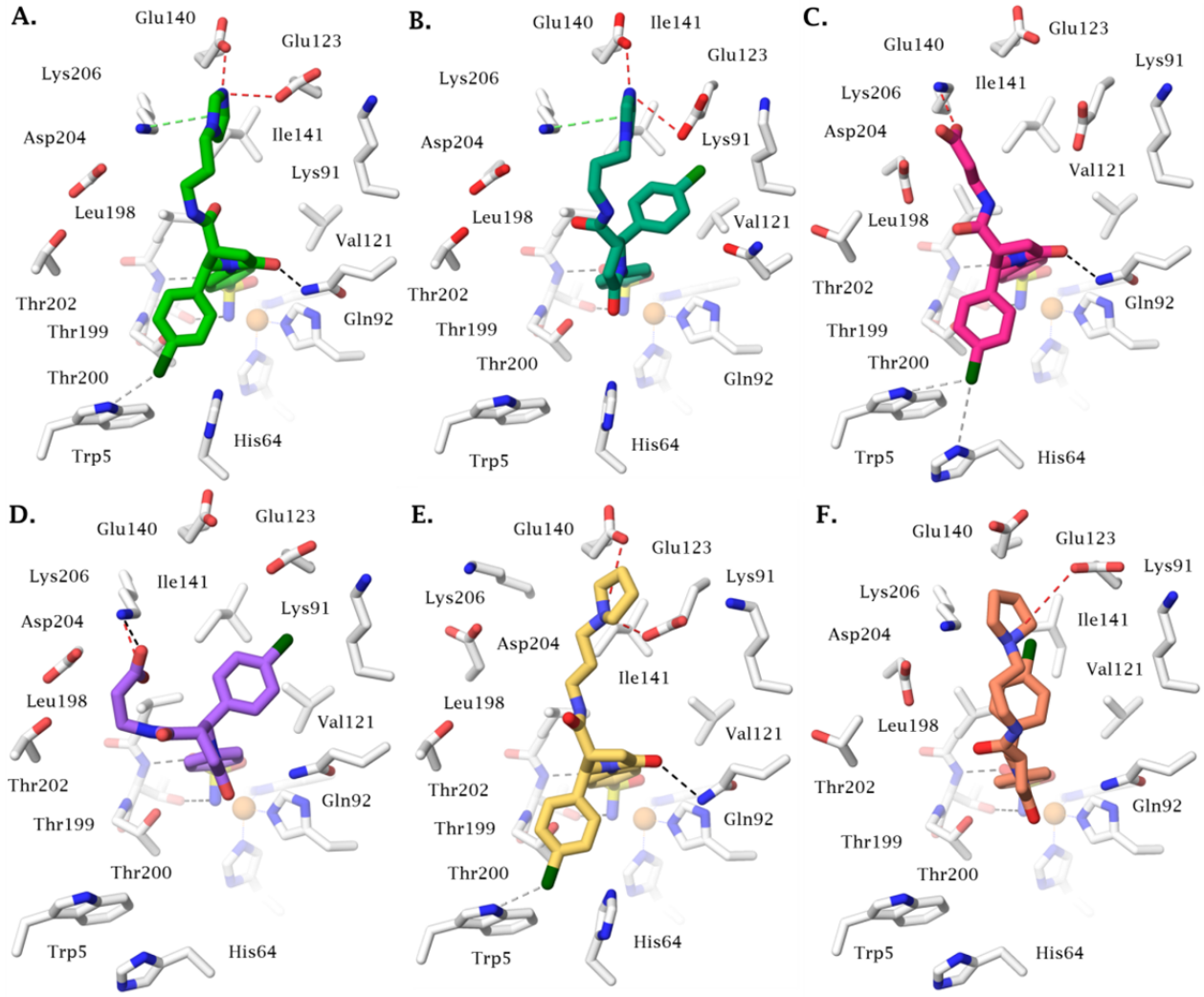

Figure 5. Induced-Fit docking of A) ***R,R*-13q**, B) ***S,S*-13q**, C) ***R,R*-13v**, D) ***S,S*-13v**, E) ***R,R*-13p**, F) ***S,S*-13p** in the *h*CA IV active site. Hydrogen bonds are represented as black dashed lines (weak ones in grey). Salt bridges are represented as red dashed lines. π-cation interactions are represented as green dashed lines.

The benzenesulfonamide fragments held the same orientation depicted for the lead molecule (**11d**) and it was not affected by the incorporation of bulkier amide residues at the methyl ester

site of **11d**. While the *S,S*-enantiomers of **13p**, **13q** and **13v** all showed a ***S,S*-11d**-like positioning for pyrrolidin-2-one and 4-chlorophenyl motifs, different lodging and interactions arose for the *R,R*-enantiomers compared to those earlier identified for ***R,R*-11d**. In the *R,R*-enantiomers, the pyrrolidin-2-one core is partially rotated, the amide carbonyl group forms an H-bond with Gln92, and the 4-chlorophenyl group is oriented towards Trp5 and His64 whose side-chain NH donate a weak H-bond to the chlorine atom.

Most importantly, the charged hydrophilic HBA/HBD groups in both enantiomers of **13p**, **13q** and **13v** incorporated to the structure of the parent ligand (**11d**) via an amide bond, were all found to point towards pocket A for both enantiomers likely driven by H-bonds and salt-bridge interactions (Figure 5). It is notable, however, that while the *R,R*-enantiomer's orientation enables these charged hydrophilic moieties to easily reach and interact with the pocket A amino acid residues, a noticeable torsion of the amidic linker is required in the case of *S,S*-enantiomers, which influences the set of interactions the charged groups can form with the protein. In particular, the positively charged imidazole ring of compound **13q**, in both conformations, forms a salt bridge with the carboxylate side chains of Glu123 and Glu140 and a π-cation interaction with the NH_3^+ of Lys206 (Figure 5A-B). The carboxylate group in the side chains of ***R,R*-/*S,S*-13v** forms a salt bridge contact with the side chain of Lys206 in two different modes depending of the ligand absolute configuration (Figure 2C-D). The protonated pyrrolidine moiety of ***R,R*-13p** is engaged in a salt-bridge contact with the carboxylates of Glu123 and Glu140 while the same pyrrolidine moiety in ***S,S*-13p** forms an interaction only with Glu123 (Figure 5E-F).

2.7. Antiproliferative activity against normal and cancer cell lines

Carbonic anhydrases in general have been considered important regulators of tumor cell pH by modulating the balance of protons and bicarbonate anions necessary to cell survival and proliferation. Of the fifteen human CA isoforms, however, only hCA IX and XII have been considered valid drug targets for cancer [54]. Other isoforms may also be considered as cancer targets, but little is known about their specific function even though there is evidence of their expression and upregulation in tumors [55]. The tumor-associated potential of *h*CA IV (particularly in brain tumors) is little studied. However, it is known that *h*CA IV mRNA expression is elevated in gliomas, renal cell carcinomas, thyroid cancers, and melanomas [56-58]. The recently noted disconnect between inhibition of *h*CA IX and XII and antiproliferative activity on cancer cells [59] also suggests that other isoforms can be implicated in the overall phenotypical cellular activity.

The six frontrunner compounds which we identified in this study as selective subnanomolar inhibitors of hCA IV (**13i, 13p, 13q, 13r, 13t** and **13v**) were screened at 30, 100 and 300 μM concentrations for their ability to affect the cell culture viability of human glioma cell line T98G [60] over non-cancerous human retinal pigment epithelial cell line ARPE-19 [61]. The experiment was performed relative to control (0 μM of the test compounds) under chemically induced (50 μM of $CoCl_2$) hypoxia [62].

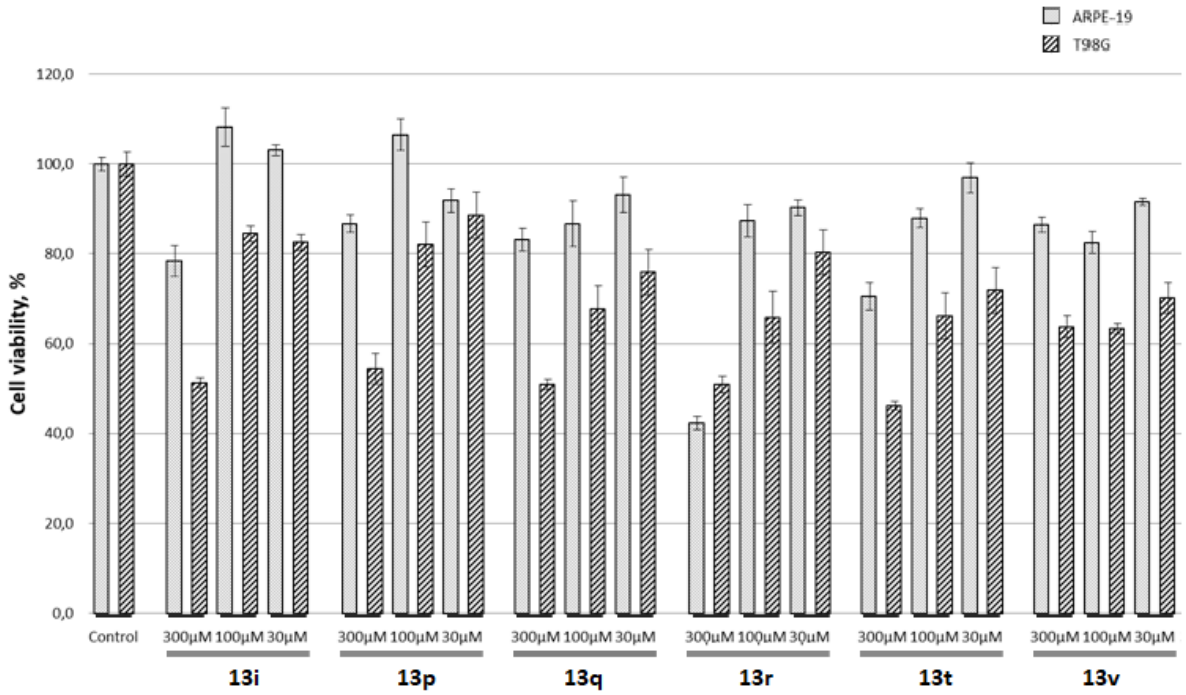

Figure 6. Cell viability MTT assay results for compounds **13i, 13p, 13q, 13r, 13t and 13v** (30, 100 and 300 μM) against ARPE-19 and T98G cell lines under hypoxic conditions (50 μM $CoCl_2$).

As it is evident from the data presented in Figure 6, virtually all compounds tested showed a cytotoxic effect towards the human glioma T98G cell line. In most cases, this effect is rather pronounced on top of unaffected viability of the normal ARPE-19 cell line (except for compound **13r** that exhibited a noticeable non-specific cytotoxicity at 300 μM). For compounds **13i** and **13p-q**, the cytotoxicity toward cancer cell line was not only selective (ARPE-19 cell viability over 80%) but also dose-dependent.

In order to link the observed cytotoxic effect toward the glioma T98G cell line to the inhibition of *h*CA IV, we were curious if there were any changes in the *h*CA IV mRNA expression under the chemically induced hypoxia condition in the same cell culture.

2.8.Evaluation of hCAIV mRNA expression in T98G cells

In order to study *h*CAIV mRNA expression in T98G cells under hypoxic conditions quantitative real-time RT-PCR measurements were performed (Figure 7).

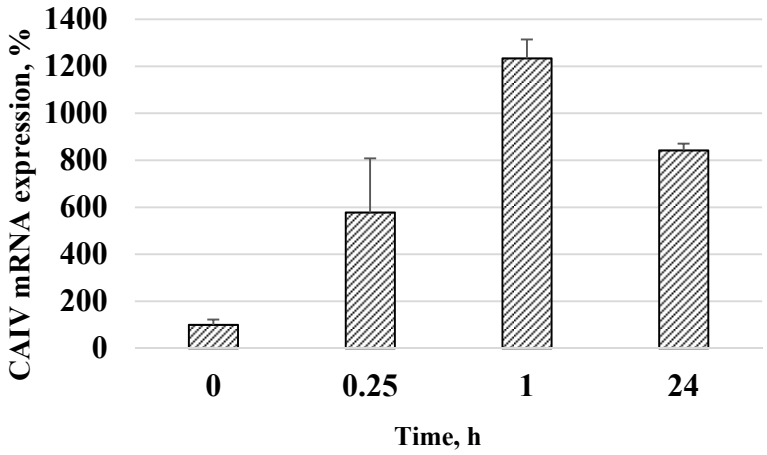

Figure 4. Time-resolved *h*CAIV mRNA expression (qPCR) profile of T98G under hypoxic conditions (100 μM $CoCl_2$).

The results indicated that *h*CAIV mRNA expression in T98G cell line markedly increased when exposed to chemically induced hypoxic conditions. Particularly, after 15 min of hypoxia the level of *h*CAIV mRNA was found to be 6 times higher in comparison to starting conditions. Moreover, after 60 min 12-fold expression was observed. These results support the idea that *h*CAIV inhibitory profile of the investigated compounds may be linked to the cytotoxic effect they exhibited against T98G cells under hypoxic conditions.

3. Conclusion

We presented a novel approach to the discovery of selective, subnanomolar inhibitors of human carbonic anhydrase IV which can be considered a target for brain cancer. Mindful of the limitation in applying target-based predictive approaches to the *de novo* design of isoform-selective inhibitors, we took a diversity-based approach. Harnessing the power of the Castagnoli-Cushman multicomponent reaction, we created a set of primary sulfonamides with varying cores as well as periphery, thus probing into fairly distant areas of the chemical space. The initial structure-activity relationships ('seed SAR') obtained after inhibition profiling of this first-iteration set of compounds revealed a low-nanomolar (albeit non-selective) inhibitor **11d**. Detailed scrutiny of the docking poses of this inhibitor revealed the presence of a hydrophilic pocket which is unique to *h*CA IV. It was pointed to by the carboxylic ester function of **11d** and therefore it was decided to decorate the core of the latter with various groups capable of forming hydrogen bonds as well as salt bridges, attached *via* a carboxamide linkage at the same carboxylic group. The second-iteration inhibitors had a remarkably improved profile toward *h*CA IV both in terms of potency and selectivity and the correctness of the design approach was corroborated by the docking study of several frontrunner compounds. The latter showed a

selective, dose-dependent cytotoxicity against human glioma T98G cell line under chemically induced hypoxia conditions. This effect may be related to the inhibition of *h*CA IV by these compounds, considering the experimentally established increased mRNA expression of this enzyme under the hypoxic conditions.

These findings substantially enrich the arsenal of available tool compounds to further elucidate the role of *h*CA IV as drug target, particularly for the treatment of glioma. The approach described also illustrate the power of multicomponent chemistry (hitherto underutilized in the field of carbonic anhydrase inhibitors) in the generation of initial leads for subsequent development of isoform-selective inhibitors. As demonstrated, with the actual leads at hand, their target-based optimization becomes far more productive compared to the attempts to target specific isoforms with new chemotype by a priori *in silico* focusing described in the literature.

4. Experimental section

4.1. General experimental

All and reagents and solvents were obtained from commercial sources and used without purification. All reactions implemented in an open flask without any protection from CO_2 and H_2O. Reactions were monitored by analytical thin layer chromatography (TLC) Macherey-Nagel, TLC plates Polygram® Sil G/UV254. Visualization of the developed chromatograms was performed by fluorescence quenching at 254 nm. ^{1}H and ^{13}C NMR spectra were measured on Bruker AVANCE DPX 400 (400 MHz for ^{1}H and 100 MHz for ^{13}C respectively). All chemical shifts (δ ppm) are given in parts per million (ppm) with reference to solvent residues in DMSO-d6-*d6* (2.50 for proton and 39.52 for carbon) and coupling constant (*J)* are reported in hertz (Hz). Multiplicities are abbreviated as follows: s = singlet, d = doublet, t = triplet, q = quartet, m = multiplet, br = broad. Melting points were determined on Electrothermal IA 9300 series Digital Melting Point Apparatus. Mass spectra were recorded on microTOF spectrometers (ESI ionization).

*4.2.1. General procedure (GP 1) for the synthesis of imines **6a-m***

A mixture of appropriate amine (0.20 mmol) and aldehyde (0.20 mmol) in 50 mL of methanol was stirred at 60°C for 4 hours in presence of catalytic amounts of *p*-toluenesulfonic acid. The reaction was cooled and the resulting precipitate was filtered and washed by 10 mL of ice-cooled isopropanol providing pure imine **6a-m** in high yields.

*4.2.1.1. 1-(4-(Benzylthio)phenyl)-N-(4-methoxyphenyl)methanimine (**6a**)*

Yield 562 mg (84%). White solid, m.p. 112-115°C ^{1}H NMR (400 MHz, Chloroform-*d*) δ 8.44 (s, 1H), 7.80 (d, J = 8.1 Hz, 2H), 7.42 – 7.37 (m, 4H), 7.36 – 7.28 (m, 3H), 7.28 – 7.23 (m, 2H), 6.96 (d, J = 8.9 Hz, 2H), 4.23 (s, 2H), 3.86 (s, 3H) ppm.

*4.2.1.2. 1-(4-(Benzylthio)phenyl)-N-(4-chlorophenyl)methanimine (**6b**)*

Yield 544 mg (81%). Yellow solid, m.p. 133-136°C ^{1}H NMR (400 MHz, Chloroform-*d*) δ 8.38 (s, 1H), 7.79 (d, J = 7.9 Hz, 2H), 7.46 – 7.28 (m, 9H), 7.16 (d, J = 8.2 Hz, 2H), 4.24 (s, 2H) ppm.

*4.2.1.2. 1-(4-(Benzylthio)phenyl)-N-(4-bromophenyl)methanimine (**6c**)*

Yield 580 mg (76%). Yellow solid, m.p. 134-137°C. ^{1}H NMR (400 MHz, Chloroform-*d*) δ 8.38 (s, 1H), 7.79 (d, J = 8.0 Hz, 2H), 7.52 (d, J = 8.2 Hz, 2H), 7.41 – 7.25 (m, 7H), 7.10 (d, J = 8.2 Hz, 2H), 4.24 (s, 2H) ppm.

*4.2.1.3**.** 1-(4-(Benzylthio)phenyl)-N-ethylmethanimine (**6d**)*

Yield 435 mg (85%). Yellow solid, m.p. 119-122°C. ^{1}H NMR (400 MHz, Chloroform-*d*) δ 8.25 (s, 1H), 7.63 (d, J = 8.3 Hz, 2H), 7.47 – 7.15 (m, 7H), 4.19 (s, 2H), 3.65 (qd, J = 7.3, 1.4 Hz, 2H), 1.32 (t, J = 7.3 Hz, 3H) ppm.

*4.2.1.4. 1-(4-(Benzylthio)phenyl)-N-isopropylmethanimine (**6e**)*

Yield 447 mg (83%). White solid, m.p. 95-98°C. ^{1}H NMR (400 MHz, Chloroform-d) δ 8.26 (s, 1H), 7.63 (d, J = 8.4 Hz, 2H), 7.36 – 7.30 (m, 6H), 7.28 – 7.24 (m, 1H), 4.18 (s, 2H), 3.54 (p, J = 6.3 Hz, 1H), 1.28 (d, J = 6.3 Hz, 6H) ppm.

*4.2.1.5. 1-(4-(Benzylthio)phenyl)-N-(3,4-dichlorophenyl)methanimine (**6f**)*

Yield 494 mg (66%). White solid, m.p. 122-125°C. ^{1}H NMR (400 MHz, Chloroform-*d*) δ 8.36 (s, 1H), 7.82 – 7.75 (m, 2H), 7.46 (d, J = 8.5 Hz, 1H), 7.43 – 7.25 (m, 8H), 7.07 (dd, J = 8.5, 2.4 Hz, 1H), 4.24 (s, 2H) ppm.

*4.2.1.6. 1-(4-(Benzylthio)phenyl)-N-(p-tolyl)methanimine (**6g**)*

Yield 525 mg (83%). White solid, m.p. 135-138°C. ^{1}H NMR (400 MHz, Chloroform-*d*) δ 8.43 (s, 1H), 7.83 (d, J = 7.9 Hz, 2H), 7.37 (d, J = 8.3 Hz, 2H), 7.36 – 7.24 (m, 7H), 7.16 (d, J = 8.3 Hz, 2H), 4.15 (s, 2H), 2.46 (s, 3H) ppm.

*4.2.1.7. N-(4-(Benzylthio)phenyl)-1-phenylmethanimine (**6h**)*

Yield 536 mg (88%). White solid, m.p. 124-127°C. ^{1}H NMR (400 MHz, Chloroform-*d*) δ 8.47 (s, 1H), 7.97 – 7.88 (m, 2H), 7.54 – 7.49 (m, 3H), 7.40 – 7.36 (m, 2H), 7.35 – 7.31 (m, 4H), 7.31 – 7.26 (m, 1H), 7.21 – 7.15 (m, 2H), 4.15 (s, 2H) ppm.

*4.2.1.8. N-(4-(Benzylthio)phenyl)-1-(p-tolyl)methanimine (**6i**)*

Yield 547 mg (86%). White solid, m.p. 105-108°C. ^{1}H NMR (400 MHz, Chloroform-*d*) δ 8.43 (s, 1H), 7.82 (d, *J* = 7.9 Hz, 2H), 7.36 (d, *J* = 8.4 Hz, 2H), 7.35 – 7.23 (m, 7H), 7.15 (d, *J* = 8.4 Hz, 2H), 4.14 (s, 2H), 2.45 (s, 3H) ppm.

*4.2.1.9. N-(4-(Benzylthio)phenyl)-1-(4-chlorophenyl)methanimine (**6j**)*

Yield 580 mg (86%). White solid, m.p. 133-136°C. ^{1}H NMR (400 MHz, Chloroform-*d*) δ 8.43 (s, 1H), 7.89 – 7.82 (m, 2H), 7.51 – 7.44 (m, 2H), 7.38 – 7.34 (m, 2H), 7.32 – 7.24 (m, 5H), 7.17 – 7.10 (m, 2H), 4.14 (s, 2H) ppm.

*4.2.1.10. N-(4-(Benzylthio)phenyl)-1-(4-fluorophenyl)methanimine (**6k**)*

Yield 532 mg (83%). White solid, m.p. 130-133°C. ^{1}H NMR (400 MHz, Chloroform-*d*) δ 8.43 (s, 1H), 7.96 – 7.87 (m, 2H), 7.39 – 7.34 (m, 2H), 7.33 – 7.24 (m, 5H), 7.22 – 7.11 (m, 4H), 4.14 (s, 2H) ppm.

*4.2.1.11. N-(4-(Benzylthio)phenyl)-1-(4-methoxyphenyl)methanimine (**6l**)*

Yield 580 mg (87%). White solid, m.p. 110-113°C. ^{1}H NMR (400 MHz, Chloroform-*d*) δ 8.40 (s, 1H), 7.87 (d, *J* = 8.3 Hz, 2H), 7.38 – 7.33 (m, 2H), 7.32 – 7.24 (m, 5H), 7.14 (d, *J* = 8.0 Hz, 2H), 7.01 (d, *J* = 8.5 Hz, 2H), 4.13 (s, 2H), 3.90 (s, 3H) ppm.

*4.2.1.12. N-(4-(Benzylthio)phenyl)-1-(3,4-dichlorophenyl)methanimine (**6m**)*

Yield 537 mg (72%). White solid, m.p. 117-120°C. ^{1}H NMR (400 MHz, Chloroform-*d*) δ 8.39 (s, 1H), 8.03 (d, *J* = 1.8 Hz, 1H), 7.72 (dd, *J* = 8.3, 1.8 Hz, 1H), 7.57 (d, *J* = 8.3 Hz, 1H), 7.38 – 7.34 (m, 2H), 7.33 – 7.30 (m, 4H), 7.28 – 7.24 (m, 1H), 7.20 – 7.11 (m, 2H), 4.15 (s, 2H) ppm.

*4.2.2. General procedure (GP 2) for the synthesis of lactams (**8a-h**, **9a-h**)*

Imine **6a-m** (1.2 mmol) and corresponding anhydride **7a-c** (1.2 mmol) were mixed in a dry reaction tube. Closed tube was heated in oil bath at 150°C for 16 hours. Then the reaction was cooled and the resulting mass was dissolved in methanol (5 mL). The solution was cooled in ice bath and $SOCl_2$ (3.0 mmol) was added dropwise. The reaction was stirred for 30 minutes then

warmed to ambient temperature followed by refluxing overnight. The reaction course was monitored by HPLC. After the reaction completion the solution was concentrated in vacuo and the residue was dissolved in DCM (20 mL), washed with H_2O (5 mL), saturated aqueous solution of Na_2CO_3 (5 mL) and brine (5 mL) and dried over Na_2SO_4. After filtration and evaporation of DCM the product was purified chromatographically to provide compounds **8a-h**, **9a-h** in 17 to 33% yields.

*4.2.2.1. trans/cis-Methyl-2-(4-(benzylthio)phenyl)-1-(4-methoxyphenyl)-5-oxopyrrolidine-3-carboxylate (**8a**)*

Yield 168 mg (31%). Yellow oil. dr: 6:1. ^{1}H NMR (400 MHz, Chloroform-*d*) δ 7.30 – 7.25 (m, 5H), 7.25 – 7.22 (m, 4H), 7.17 – 7.11 (m, 2H), 6.82 – 6.78 (m, 2H), 5.41 (d, J = 5.2 Hz, 1H), 4.09 (s, 2H), 3.79 (s, 3H), 3.76 (s, 3H), 3.13 (ddd, J = 9.2, 7.1, 5.2 Hz, 1H), 3.01 (dd, J = 17.2, 9.2 Hz, 1H), 2.93 (dd, J = 17.2, 7.1 Hz, 1H) ppm. ^{13}C NMR (100 MHz, Chloroform-*d*) δ 172.6, 171.8, 157.3, 137.7, 137.0, 136.9, 129.9, 129.0, 128.8, 128.5, 127.3, 127.0, 124.8, 114.1, 65.8, 51.9, 46.3, 38.7, 34.3, 28.9 ppm. HRMS (ESI), m/z calcd for $C_{26}H_{26}NO_4S^+$ $[M+H]^+$ 448.1577, found 448.1578.

*4.2.2.2. trans/cis-Methyl 2-(4-(benzylthio)phenyl)-1-(4-chlorophenyl)-5-oxopyrrolidine-3-carboxylate (**8b**)*

Yield 152 mg (24%). Yellow oil. dr: 7:1. ^{1}H NMR (400 MHz, Chloroform-*d*) δ 7.37 – 7.32 (m, 2H), 7.29 – 7.25 (m, 5H), 7.24 – 7.20 (m, 4H), 7.16 – 7.10 (m, 2H), 5.48 (d, J = 5.1 Hz, 1H), 4.09 (s, 2H), 3.77 (s, 3H), 3.12 (ddd, J = 9.0, 7.0, 5.1 Hz, 1H), 3.01 (dd, J = 17.3, 9.0 Hz, 1H), 2.93 (dd, J = 17.3, 7.0 Hz, 1H) ppm. ^{13}C NMR (100 MHz, Chloroform-*d*) δ 172.4, 171.9, 137.2, 137.1, 137.0, 136.0, 130.6, 129.9, 128.9, 128. 8, 128.5, 127.3, 126.7, 123.8, 65.2, 52.7, 46.2, 38.5, 34.3 ppm. HRMS (ESI), m/z calcd for $C_{25}H_{23}ClNO_3S^+$ $[M+H]^+$ 452.1082, found 452.1090.

*4.2.2.3. trans/cis-Methyl 2-(4-(benzylthio)phenyl)-1-(4-bromophenyl)-5-oxopyrrolidine-3-carboxylate (**8c**)*

Yield: 150 mg (25%). Brown oil. dr: 5:1. ^{1}H NMR (400 MHz, Chloroform-*d*) δ 7.41 – 7.35 (m, 4H), 7.29 (d, J = 6.0 Hz, 3H), 7.25 – 7.20 (m, 4H), 7.16 – 7.11 (m, 2H), 5.47 (d, J = 5.1 Hz, 1H), 4.09 (s, 2H), 3.78 (s, 3H), 3.12 (ddd, J = 9.0, 7.1, 5.1 Hz, 1H), 3.01 (dd, J = 17.3, 9.0 Hz, 1H), 2.93 (dd, J = 17.3, 7.1 Hz, 1H) ppm. ^{13}C NMR (100 MHz, Chloroform-*d*) δ 172.4, 171.9, 137.2, 137.1, 136.9, 136.5, 131.8, 129.9, 128.8, 128.5, 127.3, 126.7, 124.1, 118.5, 65.1, 52.8, 46.2, 38.6, 34.3 ppm. HRMS (ESI), m/z calcd for $C_{25}H_{23}BrNO_3S^+$ $[M+H]^+$ 496.0577, found 496.0579.

*4.2.2.4. trans/cis-Methyl 2-(4-(benzylthio)phenyl)-1-ethyl-5-oxopyrrolidine-3-carboxylate (**8d**)*

Yield 124 mg (28%). Brown oil. dr: 6:1. ^{1}H NMR (400 MHz, Chloroform-*d*) δ 7.34 – 7.29 (m, 6H), 7.27 – 7.23 (m, 1H), 7.15 (d, J = 8.3 Hz, 2H), 4.87 (d, J = 5.9 Hz, 1H), 4.15 (s, 2H), 3.73 (s, 3H), 3.79 – 3.64 (m, 1H), 3.02 (ddd, J = 9.7, 7.8, 5.9 Hz, 1H), 2.83 (dd, J = 17.1, 9.7, Hz, 1H), 2.74 (dd, J = 17.1, 7.8 Hz, 1H), 2.69 – 2.62 (m, 1H), 1.00 (t, J = 7.3 Hz, 3H) ppm. ^{13}C NMR (100 MHz, Chloroform-*d*) δ 172.7, 172.2, 137.3, 137.3, 137.0, 129.8, 128.8, 128.5, 127.3, 127.3, 63.4, 52.5, 46.1, 38.6, 35.6, 33.9, 12.0 ppm. HRMS (ESI), m/z calcd for $C_{21}H_{24}NO_3S^+$ $[M+H]^+$ 370.1471, found 370.1476.

*4.2.2.5. trans-Methyl 2-(4-(benzylthio)phenyl)-1-isopropyl-5-oxopyrrolidine-3-carboxylate (**8e**)*

Yield 115 mg (25%). Yellow oil. ^{1}H NMR (400 MHz, Chloroform-*d*) δ 7.31 – 7.29 (m, 2H), 7.29 – 7.27 (m, 4H), 7.27 – 7.24 (m, 1H), 7.19 – 7.16 (m, 2H), 4.92 (d, J = 3.8 Hz, 1H), 4.13 (s, 2H), 4.05 (p, J = 6.9 Hz, 1H), 3.74 (s, 3H), 3.00 – 2.90 (m, 1H), 2.88 (dd, J = 16.5, 9.6 Hz, 1H), 2.69 (dd, J = 16.5, 4.5 Hz, 1H), 1.22 (d, J = 6.8 Hz, 3H), 0.92 (d, J = 6.8 Hz, 3H) ppm. ^{13}C NMR (100 MHz, Chloroform-*d*) δ 172.9, 172.7, 139.7, 137.1, 136.8, 130.1, 128.8, 128.5, 127.3, 127.0, 62.8, 52.5, 46.5, 45.3, 38.8, 33.8, 20.7, 19.7 ppm. HRMS (ESI), m/z calcd for $C_{22}H_{26}NO_3S^+$ $[M+H]^+$ 384.1628, found 384.1632.

*4.2.2.6. trans/cis-Methyl 3-(4-(benzylthio)phenyl)-4-isopropyl-1-(methylsulfonyl)-5-oxopiperazine-2-carboxylate (**8f**)*

Yield 104 mg (18%). Brown oil. dr: 10:1. ^{1}H NMR (400 MHz, Chloroform-*d*) δ 7.33 (d, J = 8.3 Hz, 2H), 7.28 – 7.19 (m, 5H), 7.15 (d, J = 8.2 Hz, 2H), 5.12 (d, J = 2.2 Hz, 1H), 4.78 (dq, J = 14.3, 7.2 Hz, 1H), 4.65 (d, J = 2.2 Hz, 1H), 4.27 – 4.17 (m, 2H), 4.13 (s, 2H), 3.86 (s, 3H), 2.57 (s, 3H), 1.13 (d, J = 6.7 Hz, 3H), 0.87 (d, J = 7.0 Hz, 3H) ppm. ^{13}C NMR (100 MHz, Chloroform-*d*) δ 168.8, 163.7, 137.1, 137.1, 137.0, 130.2, 128.8, 128.5, 127.3, 126.5, 61.9, 57.2, 53.2, 46.4, 46.2, 38.8, 38.4, 19.8, 19.6 ppm. HRMS (ESI), m/z calcd for $C_{23}H_{29}N_2O_5S_2^+$ $[M+H]^+$ 477.1512, found 477.1517.

*4.2.2.7. trans-Methyl 3-(4-(benzylthio)phenyl)-4-(3,4-dichlorophenyl)-1-(methylsulfonyl)-5-oxopiperazine-2-carboxylate (**8g**)*

Yield 177 mg (25%). Brown oil. ^{1}H NMR (400 MHz, Acetone-d_6) δ 7.57 (d, J = 8.6 Hz, 1H), 7.49 – 7.42 (m, 3H), 7.40 (d, J = 8.6 Hz, 2H), 7.39 – 7.31 (m, 2H), 7.34 – 7.25 (m, 2H), 7.29 – 7.22 (m, 1H), 7.22 (dd, J = 8.6, 2.5 Hz, 1H), 5.67 (d, J = 2.1 Hz, 1H), 4.94 (d, J = 2.1 Hz, 1H), 4.45 (d, J = 17.3 Hz, 1H), 4.30 – 4.21 (m, 3H), 3.97 (s, 3H), 2.79 (s, 3H) ppm. ^{13}C NMR (100

MHz, Acetone-d_6) δ 169.0, 163.6, 141.0, 137.5, 135.3, 131.8, 130.8, 130.6, 129.3, 129.0, 128.9, 128.4, 127.5, 127.1, 126.7, 64.7, 61.1, 52.9, 46.1, 38.1, 37.5 ppm. HRMS (ESI), m/z calcd for $C_{26}H_{25}Cl_2N_2O_5S_2^+$ $[M+H]^+$ 579.0576, found 579.0578.

*4.2.2.8. trans-Methyl 3-(4-(benzylthio)phenyl)-4-isopropyl-5-oxomorpholine-2-carboxylate (**8h**)*

Yield 86 mg (18%). Brown oil. ^{1}H NMR (400 MHz, Chloroform-*d*) δ 7.31 (d, J = 8.3 Hz, 2H), 7.30 – 7.21 (m, 5H), 7.18 (d, J = 8.4 Hz, 2H), 4.94 (d, J = 1.7 Hz, 1H), 4.76 – 4.63 (m, 2H), 4.42 – 4.32 (m, 2H), 4.13 (s, 2H), 3.83 (s, 3H), 1.14 (d, J = 6.9 Hz, 3H), 0.86 (d, J = 6.9 Hz, 3H) ppm. ^{13}C NMR (100 MHz, Chloroform-*d*) δ 169.7, 165.7, 137.8, 137.1, 136.9, 129.9, 128.8, 128.5, 127.3, 127.0, 65.0, 56.4, 52.7, 46.2, 38.8, 30.9, 19.9, 19.5 ppm. HRMS (ESI), m/z calcd for $C_{22}H_{26}NO_4S^+$ $[M+H]^+$ 400.1577, found 400.1577.

*4.2.2.9. trans/cis-Methyl 1-(4-(benzylthio)phenyl)-5-oxo-2-(p-tolyl)pyrrolidine-3-carboxylate (**9a**)*

Yield 146 mg (28%). Yellow oil. dr: 7:1. ^{1}H NMR (400 MHz, Chloroform-*d*) δ 7.34 – 7.30 (m, 2H), 7.29 – 7.22 (m, 5H), 7.21 – 7.18 (m, 2H), 7.15 – 7.12 (m, 4H), 5.48 (d, J = 4.8 Hz, 1H), 4.04 (s, 2H), 3.79 (s, 3H), 3.13 (ddd, J = 9.0, 6.6, 4.8 Hz, 1H), 3.02 (dd, J = 17.2, 9.0 Hz, 1H), 2.94 (dd, J = 17.2, 6.6 Hz, 1H), 2.33 (s, 3H) ppm. ^{13}C NMR (100 MHz, Chloroform-*d*) δ 172.7, 172.0, 138.1, 137.4, 136.4, 136.2, 132.8, 130.5, 129.8, 128.8, 128.4, 127.1, 126.0, 122.9, 65.5, 52.7, 46.4, 39.4, 34.4, 21.1 ppm. HRMS (ESI), m/z calcd for $C_{26}H_{26}NO_3S^+$ $[M+H]^+$ 432.1628, found 432.1633.

*4.2.2.10. trans/cis-Methyl 1-(4-(benzylthio)phenyl)-5-oxo-2-phenylpyrrolidine-3-carboxylate (**9b**)*

Yield 140 mg (28%). Yellow oil. dr: 7:1. ^{1}H NMR (400 MHz, Chloroform-*d*) δ 7.35 – 7.30 (m, 4H), 7.26 – 7.17 (m, 10H), 5.53 (d, J = 4.7 Hz, 1H), 4.03 (s, 2H), 3.80 (s, 3H), 3.15 (ddd, J = 9.1, 6.6, 4.7 Hz, 1H), 3.03 (dd, J = 17.3, 9.1 Hz, 1H), 2.95 (dd, J = 17.3, 6.6 Hz, 1H) ppm. ^{13}C NMR (100 MHz, Chloroform-*d*) δ 172.6, 172.0, 139.5, 137.3, 136.1, 132.9, 130.6, 129.2, 128.8, 128.5, 128.3, 127.1, 126.1, 122.8, 65.6, 52.7, 46.3, 39.4, 34.3 ppm. HRMS (ESI), m/z calcd for $C_{25}H_{24}NO_3S^+$ $[M+H]^+$ 418.1471, found 418.1476.

*4.2.2.11. trans/cis-Methyl 1-(4-(benzylthio)-3-methoxyphenyl)-5-oxo-2-phenylpyrrolidine-3-carboxylate (**9c**)*

Yield 179 (33%). Yellow oil. dr: 10:1. ^{1}H NMR (400 MHz, Chloroform-*d*) δ 7.30 (d, J = 2.2 Hz, 1H), 7.28 – 7.21 (m, 6H), 6.88 – 6.82 (m, 2H), 7.17 – 7.12 (m, 2H), 6.88 – 6.82 (m, 2H), 5.45 (d, J = 5.0 Hz, 1H), 4.04 (s, 2H), 3.79 (s, 3H), 3.79 (s, 3H) 3.13 (ddd, J = 9.2, 7.0, 5.0 Hz, 1H), 3.02 (dd, J = 17.5, 9.4 Hz, 1H), 2.95 (dd, J = 17.5, 7.0 Hz, 1H) ppm. ^{13}C NMR (100 MHz, Chloroform-*d*) δ 172.6, 171.9, 159.5, 137.3, 136.1, 132.9, 131.3, 130.5, 128.8, 128.4, 127.4, 127.1, 123.1, 114.5, 65.3, 55.3, 52.6, 46.5, 39.4, 34.4 ppm. HRMS (ESI), m/z calcd for $C_{26}H_{26}NO_4S^+$ $[M+H]^+$ 448.1577, found 448.1578.

*4.2.2.12. trans/cis-Methyl 1-(4-(benzylthio)phenyl)-2-(4-chlorophenyl)-5-oxopyrrolidine-3-carboxylate (**9d**)*

Yield 162 (30%). Yellow oil. dr: 7:1. ^{1}H NMR (400 MHz, Chloroform-*d*) δ 7.31 (d, J = 8.3 Hz, 2H), 7.27 – 7.15 (m, 11H), 5.50 (d, J = 5.1 Hz, 1H), 4.05 (s, 2H), 3.80 (s, 3H), 3.11 (ddd, J = 9.2, 7.5, 5.2 Hz, 1H), 3.02 (dd, J = 17.5, 9.2 Hz, 1H), 2.95 (dd, J = 17.5, 7.5 Hz, 1H) ppm. ^{13}C NMR (100 MHz, Chloroform-*d*) δ 172.3, 171.7, 138.0, 137.2, 135.7, 134.2, 133.2, 130.6, 129.4, 128.8, 128.5, 127.6, 127.2, 122.9, 64.9, 52.8, 46.3, 39.3, 34.3 ppm. HRMS (ESI), m/z calcd for $C_{25}H_{23}ClNO_3S^+$ $[M+H]^+$ 452.1082, found 452.1090.

*4.2.2.13. trans/cis-Methyl 1-(4-(benzylthio)phenyl)-2-(4-fluorophenyl)-5-oxopyrrolidine-3-carboxylate (**9e**)*

Yield 107 mg (20%). Yellow oil. dr: 8:1. ^{1}H NMR (400 MHz, Chloroform-*d*) δ 7.35 – 7.29 (m, 3H), 7.27 – 7.13 (m, 10H), 5.50 (d, J = 5.2 Hz, 1H), 4.05 (s, 2H), 3.80 (s, 3H), 3.11 (ddd, J = 9.0, 7.4, 5.2 Hz, 1H), 3.02 (dd, J = 17.2, 9.0 Hz, 1H), 2.95 (dd, J = 17.2, 7.4 Hz, 1H) ppm. ^{13}C NMR (100 MHz, Chloroform-*d*) δ 172.4, 171.8, 162.5 (d, J = 247.7 Hz), 137.3, 135.7, 135.1 (d, J = 3.3 Hz), 133.2, 130.6, 130.5, 129.0, 128.8, 128.5, 128.0 (d, J = 8.3 Hz), 127.2, 123.0, 122.3, 116.2 (d, J = 21.8 Hz), 65.0, 52.7, 46.4, 39.3, 34.3 ppm. HRMS (ESI), m/z calcd for $C_{25}H_{23}FNO_3S^+$$[M+H]^+$ 436.1377, found 436.1380.

*4.2.2.14. trans-Methyl 4-(4-(benzylthio)phenyl)-1-(methylsulfonyl)-5-oxo-3-(p-tolyl)piperazine-2-carboxylate (**9f**)*

Yield 120 mg (19%). Brown oil. ^{1}H NMR (400 MHz, Chloroform-*d*) δ 7.33 – 7.28 (m, 4H), 7.28 – 7.24 (m, 3H), 7.26 – 7.18 (m, 4H), 7.07 – 7.00 (m, 2H), 5.44 (d, J = 2.2 Hz, 1H), 4.85 (d, J = 2.2 Hz, 1H), 4.43 (d, J = 17.3 Hz, 1H), 4.34 (d, J = 17.3 Hz, 1H), 4.10 (s, 2H), 3.93 (s, 3H), 2.71 (s, 3H), 2.37 (s, 3H) ppm. ^{13}C NMR (101 MHz, Chloroform-*d*) δ 169.1, 164.0, 138.9, 138.7, 136.9, 136.7, 134.1, 129.9, 129.7, 128.7, 128.6, 127.3, 126.7, 126.3, 65.4, 61.6, 53.5, 46.3, 38.6,

38.58, 21.2 ppm. HRMS (ESI), m/z calcd for $C_{27}H_{29}N_2O_5S_2^+$ $[M+H]^+$ 525.1512, found 525.1519.

*4.2.2.15. trans-Methyl 4-(4-(benzylthio)phenyl)-3-(3,4-dichlorophenyl)-1-(methylsulfonyl)-5-oxopiperazine-2-carboxylate (**9g**)*

Yield 146 mg (21%). Brown oil. ^{1}H NMR (400 MHz, Chloroform-*d*) δ 7.52 (d, J = 8.3 Hz, 1H), 7.39 (d, J = 2.2 Hz, 1H), 7.32 – 7.20 (m, 8H), 6.96 (d, J = 8.6 Hz, 2H), 5.42 (d, J = 1.9 Hz, 1H), 4.83 (d, J = 1.9 Hz, 1H), 4.53 (d, J = 17.3 Hz, 1H), 4.28 (d, J = 17.3 Hz, 1H), 4.11 (s, 2H), 3.96 (s, 3H), 2.91 (s, 3H) ppm. ^{13}C NMR (100 MHz, Chloroform-*d*) δ 168.5, 163.6, 138.0, 137.4, 137.2, 136.7, 133.5, 133.4, 131.2, 129.7, 128.8, 128.7, 128.6, 127.4, 126.8, 125.8, 64.6, 60.8, 53.7, 46.1, 38.8, 38.4 ppm. HRMS (ESI), m/z calcd for $C_{26}H_{25}Cl_2N_2O_5S_2^+[M+H]^+$ 579.0576, found 579.0579.

*4.2.2.16. trans-Methyl 4-(4-(benzylthio)phenyl)-5-oxo-3-(p-tolyl)morpholine-2-carboxylate (**9h**)*

Yield 93 mg (17%). Brown oil. ^{1}H NMR (400 MHz, Chloroform-*d*) δ 7.35 – 7.25 (m, 5H), 7.25 – 7.21 (m, 2H), 7.21 – 7.19 (m, 4H), 7.05 (d, J = 8.5 Hz, 2H), 5.28 (d, J = 2.7 Hz, 1H), 4.77 (d, J = 17.2 Hz, 1H), 4.61 – 4.53 (m, 2H), 4.09 (s, 2H), 3.89 (s, 3H), 2.37 (s, 3H) ppm. ^{13}C NMR (100 MHz, Chloroform-*d*) δ 169.6, 166.0, 138.5, 138.2, 137.0, 136.2, 134.3, 129.9, 129.7, 128.8, 128.5, 127.3, 127.0, 126.9, 77.3, 65.5, 64.2, 52.9, 38.8, 21.1 ppm. HRMS (ESI), m/z calcd for $C_{26}H_{26}Cl_2N_2O_5S_2$ [M+H]+ 448.1577, found 448.1580.

*4.2.3. General procedure (GP 3): preparation of sulfonamide bearing lactams (**10 a-h**, **11 a-h**)*

To a cooled solution of ester **8a-h**, **9a-h** (0.20 mmol) in a mixture of acetic acid and H_2O (9:1) (5 mL) *N*-chlorosuccinimide (80 mg, 0.60 mmol). The reaction mixture was stirred at room temperature for 4 hours. The solvent was evaporated under vacuo at 35° C. The residue was dissolved in DCM (5.0 mL), washed with H_2O (3.0 mL), 10% aqueous solution of $NaHCO_3$ (3.0 mL) and brine (3.0 mL). DCM was then evaporated, the residue was washed with diethyl ester (2x3.0 mL), dissolved in acetonitrile and 33% aqueous solution of NH_3 was added (1 mL). The mixture was stirred at room temperature for 1 hour, the precipitate formed was filtered, washed with H_2O (3.0 mL) and dried under vacuo. Product **10a-h**, **11a-h** was purified by HPLC and the fraction enriched with trans-isomer was isolated.

*4.2.3.1. Methyl (2RS,3RS)-1-(4-methoxyphenyl)-5-oxo-2-(4-sulfamoylphenyl)pyrrolidine-3-carboxylate (**10a**)*

Yield 35 mg (43%). White solid, m.p. 189-192°C. ^{1}H NMR (400 MHz, DMSO-d_6) δ 7.74 (d, J = 8.4 Hz, 2H), 7.53 (d, J = 8.4 Hz, 2H), 7.30 (br.s, 2H), 7.28 (d, J = 9.0 Hz, 2H), 6.82 (d, J = 9.0 Hz, 2H), 5.60 (d, J = 6.1 Hz, 1H), 3.69 (s, 3H), 3.67 (s, 3H), 3.25 (ddd, J = 9.6, 7.5, 6.1 Hz, 1H), 2.96 (dd, J = 17.1, 9.6 Hz, 1H), 2.80 (dd, J = 17.0, 7.5 Hz, 1H) ppm. ^{13}C NMR (126 MHz, DMSO-d_6) δ 172.7, 171.9, 157.0, 144.6, 144.0, 130.6, 128.2, 126.5, 125.4, 114.2, 64.7, 55.6, 52.8, 45.6, 34.1 ppm. HRMS (ESI), m/z calcd for $C_{19}H_{21}N_2O_6S^+$ [M+H]+ 405.1115, found 405.1124.

*4.2.3.2. Methyl (2RS,3RS)-1-(4-chlorophenyl)-5-oxo-2-(4-sulfamoylphenyl)pyrrolidine-3-carboxylate (**10b**)*

Yield 40 mg (49%). White solid. dr: 7:1. m.p. 192-195°C. ^{1}H NMR (400 MHz, DMSO-d_6) δ 7.75 (d, J = 8.4 Hz, 2H), 7.54 (d, J = 8.4 Hz, 2H), 7.46 (d, J = 9.0 Hz, 2H), 7.38 (d, J = 9.0 Hz, 2H), 7.31 (br.s, 2H), 5.70 (d, J = 6.0 Hz, 1H), 3.69 (s, 3H), 3.26 (ddd, J = 9.6, 7.4, 6.0 Hz, 1H), 2.99 (dd, J = 17.2, 9.6 Hz, 1H), 2.84 (dd, J = 17.2, 7.4 Hz, 1H) ppm. ^{13}C NMR (100 MHz, DMSO-d_6) δ 173.4, 172.8, 162.8, 144.5, 137.0, 128.9, 128.0, 127.7, 126.6, 124.6, 65.0, 52.8, 46.5, 36.3 ppm. HRMS (ESI), m/z calcd for $C_{18}H_{18}ClN_2O_5S$ [M+H]+ 409.0619, found 409.0621.

*4.2.3.3. Methyl (2RS,3RS)-1-(4-bromophenyl)-5-oxo-2-(4-sulfamoylphenyl)pyrrolidine-3-carboxylate (**10c**)*

Yield 34 mg (37%). White solid, m.p. 194-197°C. ^{1}H NMR (400 MHz, DMSO-d_6) δ 7.75 (d, J = 8.4 Hz, 2H), 7.54 (d, J = 8.4 Hz, 2H), 7.46 (d, J = 9.0 Hz, 2H), 7.39 (d, J = 9.0 Hz, 2H), 7.30 (br.s, 2H), 5.70 (d, J = 5.9 Hz, 1H), 3.70 (s, 3H), 3.26 (ddd, J = 9.6, 7.3, 5.9 Hz, 1H), 2.99 (dd, J = 17.1, 9.6 Hz, 1H), 2.84 (dd, J = 17.1, 7.3 Hz, 1H) ppm. ^{13}C NMR (100 MHz, DMSO-d_6) δ 172.5, 172.2, 144.1, 144.1, 137.1, 131.9, 128.0, 126.6, 125.3, 117.8, 64.1, 52.8, 45.5, 34.3 ppm. HRMS ESI calc. for $C_{18}H_{18}BrN_2O_5S^+$ [M+H] 453.0114, found 453.0118.

*4.2.3.4. Methyl (2RS,3RS)-1-isopropyl-5-oxo-2-(4-sulfamoylphenyl)pyrrolidine-3-carboxylate (**10d**)*

Yield 26 mg (39%). White solid, m.p. 172-175°C. ^{1}H NMR (400 MHz, DMSO-d_6) δ 7.85 (d, J = 7.9 Hz, 2H), 7.58 (d, J = 8.0 Hz, 2H), 7.39 (br.s, 2H), 4.98 (d, J = 4.2 Hz, 1H), 3.88 – 3.76 (m, 1H), 3.66 (s, 3H), 3.03 (dt, J = 9.5, 4.6 Hz, 1H), 2.84 (dd, J = 16.9, 9.6 Hz, 1H), 1.13 (d, J = 6.9 Hz, 4H), 0.82 (d, J = 6.9 Hz, 3H) ppm. ^{13}C NMR (100 MHz, DMSO-d_6) δ 173.1, 172.7, 146.4, 144.3, 127.9 (2C), 126.6 (2C), 62.5, 52.7, 45.9, 45.0, 33.5, 20.8, 19.9 ppm. HRMS ESI calc. for $C_{15}H_{21}N_2O_5S$ [M+H] 341.1166, found 341.1167.

*4.2.3.5. Methyl (2RS,3RS)-1-ethyl-5-oxo-2-(4-sulfamoylphenyl)pyrrolidine-3-carboxylate (**10e**)*

Yield 30 mg (46%). Brown solid. dr: 8:1. m.p. 178-181°C. ^{1}H NMR (400 MHz, Acetone-d_6) δ 7.96 (d, J = 8.5 Hz, 2H), 7.58 (d, J = 8.4 Hz, 2H), 6.66 (br.s, 2H), 5.04 (d, J = 5.7 Hz, 1H), 3.71 (s, 3H), 3.63 (dq, J = 14.5, 7.3 Hz, 1H), 3.19 (ddd, J = 9.7, 7.3, 5.9 Hz, 1H), 2.80 (dd, J = 16.7, 9.7 Hz, 1H), 2.71 – 2.55 (m, 2H), 0.97 (t, J = 7.3 Hz, 3H) ppm. ^{13}C NMR (100 MHz, Acetone-d_6) δ 172.4, 171.7, 144.5, 144.1, 127.7, 126.7, 63.0, 51.7, 45.6, 35.2, 33.0, 11.4 ppm. HRMS ESI calc. for $C_{14}H_{19}N_2O_5S^+$ [M+H]+ 327.1009, found 327.1014.

*4.2.3.6. Methyl (2RS,3RS)-4-(3,4-dichlorophenyl)-1-(methylsulfonyl)-5-oxo-3-(4-sulfamoylphenyl)piperazine-2-carboxylate (**10f**)*

Yield 47 mg (44%). White solid, 205-208°C. ^{1}H NMR (400 MHz, Acetone-d_6) δ 7.96 (d, J = 8.4 Hz, 2H), 7.76 (d, J = 8.2 Hz, 2H), 7.59 (d, J = 8.6 Hz, 1H), 7.53 (d, J = 2.4 Hz, 1H), 7.27 (dd, J = 8.6, 2.5 Hz, 1H), 6.65 (br.s, 2H), 5.86 (d, J = 2.2 Hz, 1H), 5.04 (d, J = 2.2 Hz, 1H), 4.49 (d, J = 17.3 Hz, 1H), 4.26 (d, J = 17.3 Hz, 1H), 4.00 (s, 3H), 2.91 (s, 3H) ppm.^{13}C NMR (100 MHz, Acetone-d_6) δ 178.0, 168.8, 163.6, 144.5, 141.4, 140.7, 131.9, 130.9, 130.7, 129.2, 127.7, 126.9, 126.6, 64.6, 60.9, 53.0, 46.1, 38.0 ppm. HRMS ESI calc. for $C_{19}H_{20}Cl_2N_3O_7S_2^+$ [M+H]+ 536.0114, found 536.0119.

*4.2.3.7. Methyl (2RS,3RS)-4-isopropyl-1-(methylsulfonyl)-5-oxo-3-(4-sulfamoylphenyl) piperazine-2-carboxylate (**10g**)*

Yield 39 mg (46%). White solid. dr: 7:1. m.p. 196-199°C. ^{1}H NMR (400 MHz, DMSO-d_6) δ 7.84 (d, J = 8.1 Hz, 2H), 7.58 (d, J = 8.1 Hz, 2H), 7.40 (br.s, 2H), 5.32 (d, J = 2.4 Hz, 1H), 4.73 (d, J = 2.4 Hz, 1H), 4.59 (p, J = 6.9 Hz, 1H), 4.24 (d, J = 16.7 Hz, 1H), 4.06 (d, J = 16.7 Hz, 1H), 3.80 (s, 3H), 2.66 (s, 3H), 1.05 (d, J = 6.7 Hz, 3H), 0.78 (d, J = 6.9 Hz, 3H) ppm. ^{13}C NMR (100 MHz, DMSO-d_6) δ 169.2, 163.9, 144.2, 143.8, 127.7, 126.3, 61.3, 57.1, 53.5, 46.5, 46.4, 38.5, 19.8, 19.6 ppm. HRMS ESI calc. for $C_{16}H_{24}N_3O_7S_2^+$ $[M+H]^+$ 434.1050, found 434.1054.

*4.2.3.8. Methyl (2RS,3RS)-4-isopropyl-5-oxo-3-(4-sulfamoylphenyl)morpholine-2-carboxylate (**10h**)*

Yield 25 mg (34%). White solid, m.p. 199-202°C. ^{1}H NMR (400 MHz, Acetone-d_6) δ 7.96 (d, J = 8.4 Hz, 2H), 7.64 (d, J = 8.4 Hz, 2H), 6.62 (br.s, 2H), 5.22 (d, J = 1.5 Hz, 1H), 4.69 – 4.58 (m, 2H), 4.55 (d, J = 16.7 Hz, 1H), 4.34 (d, J = 16.7 Hz, 1H), 3.84 (s, 3H), 1.15 (d, J = 6.8 Hz, 3H), 0.88 (d, J = 6.8 Hz, 3H) ppm. ^{13}C NMR (100 MHz, Acetone-d_6) δ 169.4, 164.9, 144.8, 143.8,

127.5, 126.4, 76.7, 64.7, 56.6, 51.9, 46.0, 19.1, 18.8 ppm. HRMS ESI calc. for $C_{15}H_{21}N_2O_6S^+$ $[M+H]^+$ 357.1115, found 357.1117.

*4.2.3.9. Methyl (2RS,3RS)-5-oxo-1-(4-sulfamoylphenyl)-2-(p-tolyl)pyrrolidine-3-carboxylate (**11a**)*

Yield 34 mg (44%). White solid, m.p. 205-208°C. ^{1}H NMR (400 MHz, DMSO-d_6) δ 7.69 (d, J = 8.8 Hz, 2H), 7.60 (d, J = 8.8 Hz, 2H), 7.25 (br.s, 2H), 7.22 (d, J = 7.8 Hz, 2H), 7.11 (d, J = 7.8 Hz, 2H), 5.63 (d, J = 5.6 Hz, 1H), 3.69 (s, 3H), 3.22 (ddd, J = 9.5, 7.0, 5.6 Hz, 1H), 3.02 (dd, J = 17.2, 9.5 Hz, 1H), 2.83 (dd, J = 17.2, 7.0 Hz, 1H), 2.22 (s, 3H) ppm. ^{13}C NMR (100 MHz, DMSO-d_6) δ 172.8, 172.5, 140.8, 140.2, 137.8, 137.1, 129.9, 127.1, 126.5, 122.8, 64.5, 52.8, 45.9, 34.5, 21.1 ppm. HRMS ESI calc. for $C_{19}H_{21}N_2O_5S^+$$[M+H]^+$ 389.1166, found 389.1163.

*4.2.3.10. Methyl (2RS,3RS)-5-oxo-2-phenyl-1-(4-sulfamoylphenyl)pyrrolidine-3-carboxylate (**11b**)*

Yield 30 mg (41%). White solid, 200-203°C. ^{1}H NMR (400 MHz, Acetone-d_6) δ 7.77 (d, J = 9.0 Hz, 2H), 7.71 (d, J = 9.0 Hz, 2H), 7.43 – 7.34 (m, 4H), 7.32 – 7.27 (m, 1H), 6.45 (br.s, 2H), 5.76 (d, J = 5.0 Hz, 1H), 3.76 (s, 3H), 3.30 (ddd, J = 9.5, 6.4, 5.0 Hz, 1H), 3.06 (dd, J = 17.3, 9.5 Hz, 1H), 2.90 (dd, J = 17.3, 6.4 Hz, 1H) ppm. ^{13}C NMR (100 MHz, Acetone-d_6) δ 172.4, 172.0, 141.3, 140.1, 139.7, 139.6, 129.0, 128.1, 126.5, 121.7, 64.8, 51.9, 45.8, 33.9 ppm. HRMS (ESI), m/z calcd for $C_{18}H_{19}N_2O_5S^+$ $[M+H]^+$ 375,1009, found 375,1008.

*4.2.3.11. Methyl (2RS,3RS)-2-(4-methoxyphenyl)-5-oxo-1-(4-sulfamoylphenyl)pyrrolidine-3-carboxylate (**11c**)*

Yield 35 mg (43%). White solid, m.p. 178-181°C. ^{1}H NMR (400 MHz, DMSO-d_6) δ 7.68 (d, J = 8.8 Hz, 2H), 7.59 (d, J = 8.8 Hz, 2H), 7.27 (d, J = 8.8 Hz, 2H), 7.24 (br.s, 2H), 6.86 (d, J = 8.6 Hz, 2H), 5.61 (d, J = 5.8 Hz, 1H), 3.69 (s, 3H), 3.69 (s, 3H), 3.23 (ddd, J = 9.5, 7.2, 5.8 Hz, 1H), 3.01 (dd, J = 17.2, 9.5 Hz, 1H), 2.82 (dd, J = 17.2, 7.2 Hz, 1H) ppm. ^{13}C NMR (100 MHz, DMSO-d_6) δ 172.8, 172.4, 159.3, 140.8, 140.2, 131.8, 128.6, 126.5, 122.9, 114.6, 64.2, 55.5, 52.7, 46.0, 34.5 ppm. HRMS ESI calc. for $C_{19}H_{21}N_2O_6S^+$ $[M+H]^+$ 405,1115, found 405,1114.

*4.2.3.12. Methyl (2RS,3RS)-2-(4-chlorophenyl)-5-oxo-1-(4-sulfamoylphenyl)pyrrolidine-3-carboxylate (**11d**)*

Yield 39 mg (48%). White solid, m.p. 171-174°C. ^{1}H NMR (400 MHz, DMSO-d_6) δ 7.70 (d, J = 8.9 Hz, 2H), 7.60 (d, J = 8.9 Hz, 2H), 7.42 – 7.35 (m, 4H), 7.24 (br.s, 2H), 5.70 (d, J = 5.9 Hz,

1H), 3.69 (s, 3H), 3.27 (ddd, *J* = 9.5, 7.3, 5.8 Hz, 1H), 3.01 (dd, *J* = 17.2, 9.5 Hz, 1H), 2.85 (dd, *J* = 17.2, 7.3 Hz, 1H) ppm. ^{13}C NMR (100 MHz, Acetone-d_6) δ 172.2, 172.0, 141.0, 139.9, 139.0, 133.4, 129.0, 128.6, 126.5, 122.0, 64.1, 51.9, 45.7, 33.8 ppm. HRMS ESI calc. for $C_{18}H_{18}ClN_2O_5S^+$ [M+H] 409.0619, found 409.0619.

*4.2.3.13. Methyl (2RS,3RS)-2-(4-fluorophenyl)-5-oxo-1-(4-sulfamoylphenyl)pyrrolidine-3-carboxylate (**11e**)*

Yield 35 mg (45%). White solid, m.p. 165-168°C. ^{1}H NMR (400 MHz, Acetone-d_6) δ 7.77 (d, *J* = 8.8 Hz, 2H), 7.69 (d, *J* = 8.8 Hz, 2H), 7.48 (dd, *J* = 8.8, 5.3 Hz, 2H), 7.12 (t, *J* = 8.8 Hz, 2H), 6.46 (br.s, 2H), 5.77 (d, *J* = 5.5 Hz, 1H), 3.76 (s, 3H), 3.32 (ddd, *J* = 9.5, 6.9, 5.5 Hz, 1H), 3.06 (dd, *J* = 17.3, 9.5 Hz, 1H), 2.91 (dd, *J* = 17.3, 6.9 Hz, 1H) ppm. ^{13}C NMR (101 MHz, Acetone-d_6) δ 172.2, 171.9, 162.3 (d, *J* = 244.9 Hz), 141.1, 139.8, 136.1 (d, *J* = 3.1 Hz), 128.8 (d, *J* = 8.4 Hz), 126.5, 122.0, 115.7 (d, *J* = 21.9 Hz), 64.1, 51.9, 45.9, 33.9 ppm. HRMS (ESI), m/z calcd for $C_{18}H_{18}FN_2O_5S^+$[M+H]$^+$ 393.0915, found 393.0921.

*4.2.3.14. Methyl (2SR,3RS)-1-(methylsulfonyl)-5-oxo-4-(4-sulfamoylphenyl)-3-(p-tolyl)piperazine-2-carboxylate (**11f**)*

Yield: 42 mg (44%). White solid, 181-184°C. ^{1}H NMR (400 MHz, DMSO-d_6) δ 8.04 – 7.82 (m, 2H), 7.54 – 7.39 (m, 2H), 7.37 (br.s, 2H), 7.27 (d, *J* = 8.2 Hz, 2H), 7.21 (d, *J* = 8.2 Hz, 2H), 5.54 (d, *J* = 2.3 Hz, 1H), 4.91 (d, *J* = 2.3 Hz, 1H), 4.47 (d, *J* = 17.4 Hz, 1H), 4.17 (d, *J* = 17.4 Hz, 1H), 3.92 (s, 3H), 2.70 (s, 3H), 2.37 (s, 3H) ppm. ^{13}C NMR (101 MHz, DMSO-d_6) δ 169.4, 164.3, 144.0, 143.1, 138.2, 134.6, 129.8, 127.4, 127.2, 127.1, 64.6, 61.2, 53.8, 46.5, 38.9, 21.1 ppm. HRMS (ESI), m/z calcd for $C_{20}H_{24}N_3O_7S_2^+$[M+H]$^+$ 482.1050, found 482.1055.

*4.2.3.15. Methyl (2SR,3RS)-3-(3,4-dichlorophenyl)-1-(methylsulfonyl)-5-oxo-4-(4-sulfamoylphenyl)piperazine-2-carboxylate (**11g**)*

Yield 45 mg (42%). White solid, m.p. 204-207°C. ^{1}H NMR (400 MHz, Acetone-d_6) δ 7.89 (d, *J* = 8.7 Hz, 2H), 7.78 (d, *J* = 2.2 Hz, 1H), 7.66 (d, *J* = 8.4 Hz, 1H), 7.57 (dd, *J* = 8.4, 2.2 Hz, 1H), 7.46 (d, *J* = 8.7 Hz, 2H), 6.60 (br.s, 2H), 5.81 (d, *J* = 2.2 Hz, 1H), 5.05 (d, *J* = 2.2 Hz, 1H), 4.53 (d, *J* = 17.4 Hz, 1H), 4.26 (d, *J* = 17.4 Hz, 1H), 3.99 (s, 3H), 2.99 (s, 3H) ppm. ^{13}C NMR (100 MHz, Acetone-d_6) δ 168.7, 163.5, 144.0, 143.0, 138.7, 132.3, 132.0, 130.9, 129.4, 127.3, 127.2, 127.1, 63.9, 60.7, 53.0, 46.1, 38.2 ppm. HRMS (ESI), m/z calcd for $C_{19}H_{20}Cl_2N_3O_7S_2^+$ [M+H]$^+$ 536.0114, found 536.0120.

*4.2.3.16. Methyl (2RS,3RS)-5-oxo-4-(4-sulfamoylphenyl)-3-(p-tolyl)morpholine-2-carboxylate (**11h**)*

Yield: 34 mg (42%). White solid, m.p. 197-200°C. ^{1}H NMR (400 MHz, DMSO-d_6) δ 7.77 (d, J = 8.4 Hz, 2H), 7.41 (d, J = 8.4 Hz, 2H), 7.34 (br.s, 2H), 7.29 (d, J = 7.9 Hz, 2H), 7.16 (d, J = 7.9 Hz, 2H), 5.46 (d, J = 3.7 Hz, 1H), 4.81 (d, J = 3.7 Hz, 1H), 4.63 (d, J = 16.7 Hz, 1H), 4.48 (d, J = 16.7 Hz, 1H), 3.77 (s, 3H), 2.26 (s, 3H) ppm. ^{13}C NMR (100 MHz, DMSO-d_6) δ 171.3, 166. 8, 158.2, 137.3, 137.0, 134.2, 129.6, 128.4, 127.4, 114.4, 78.5, 65.2, 64.9, 55.7, 21.1 ppm. HRMS (ESI), m/z calcd for $C_{19}H_{21}N_2O_6S^+$ $[M+H]^+$ 405.1115, found 405.1125.

*4.2.4. (2RS,3RS)-2-(4-Chlorophenyl)-5-oxo-1-(4-sulfamoylphenyl)pyrrolidine-3-carboxylic acid (**12**)*

$LiOHxH_2O$ (185 mg, 4.40 mmol) was dissolved in H_2O (2.0 mL) and added to a solution of **11d** (600 mg, 1.47 mmol) in methanol. The mixture was stirred overnight at 60°C. The course of the reaction was monitored by TLC. After the reaction completion 10% aqueous solution of HCl was added to reduce the pH level of the mixture to 3. The product was extracted using ethyl acetate (10 mL), washed with H_2O (3x5 mL), dried over Na_2SO_4, filtered and concentrated in vacuo to afford 504 mg (87%) of tittle compound as white solid. m.p. 188-191°C ^{1}H NMR (400 MHz, Acetone-d_6) δ 11.30 (br.s, 1H), 7.82 – 7.76 (m, 2H), 7.74 – 7.68 (m, 2H), 7.50 – 7.44 (m, 2H), 7.43 – 7.36 (m, 2H), 6.47 (br.s, 2H), 5.79 (d, J = 5.4 Hz, 1H), 3.32 (ddd, J = 9.5, 6.9, 5.4 Hz, 1H), 3.09 (dd, J = 17.3, 9.5 Hz, 1H), 2.94 (dd, J = 17.3, 6.9 Hz, 1H) ppm. ^{13}C NMR (100 MHz, Acetone-d_6) δ 172.6, 172.2, 141.1, 139.8, 139.1, 133.4, 129.0, 128.6, 126.6, 122.0, 64.3, 45.6, 34.0 ppm. HRMS (ESI), m/z calcd for $C_{17}H_{16}ClN_2O_5S^+$ $[M+H]^+$ 395,0463, found 395,0467.

4.2.5. General procedure (GP 4) for the synthesis amide derivatives (**13a-r)**.

Into a well dried flask acid **9** (80 mg, 0.20 mmol) was loaded and dissolved in dry DMF (3.0 mL). Solution of 1,1'-carbonyldiimidazole (38 mg, 0.23 mmol) in DMF (1.0 mL) was added and the mixture was stirred for 1 hour. The solution of corresponding amine (0.27 mmol) in dry DMF (1.0 mL) was added slowly. In case the amine reagent was stored as hydrochloride form, its solution was preliminary treated with TEA (0.30 mmol) and then added to the reaction flask. The mixture was stirred overnight, concentrated in vacuo. The residue was dissolved in ethyl acetate (5 mL), washed with H_2O (3x5mL) and brine (3x5mL), dried over Na_2SO_4 and the solvent was removed using rotary evaporator. In case of need product was then purified by HPLC.

*4.2.5.1. (2RS,3RS)2-(4-Chlorophenyl)-5-oxo-1-(4-sulfamoylphenyl)pyrrolidine-3-carboxamide (**13a**)*

Yield: 36 mg (45%). White solid, m.p. 185-188°C. ^{1}H NMR (400 MHz, DMSO-d_6) δ 7.69 (d, J = 8.9 Hz, 2H), 7.62 (d, J = 8.9 Hz, 2H), 7.55 (s, 1H), 7.38 (d, J = 8.7 Hz, 2H), 7.34 (d, J = 8.7 Hz, 2H), 7.23 (br.s, 2H), 7.17 (s, 1H), 5.59 (d, J = 4.9 Hz, 1H), 3.02 – 2.88 (m, 2H), 2.74 – 2.61 (m, 1H) ppm. ^{13}C NMR (100 MHz, DMSO-d_6) δ 173.4, 173.1, 140.8, 140.1, 139.5, 132.9, 129.2, 129.1, 126.6, 122.5, 64.7, 46.5, 35.5 ppm. HRMS (ESI), m/z calcd for $C_{17}H_{17}ClN_3O_4S^+$ $[M+H]^+$ 394.0623, found 394.0626.

*4.2.5.2. 4-((2RS,3RS)-(2-(4-Chlorophenyl)-5-oxo-3-(pyrrolidine-1-carbonyl)pyrrolidin-1-yl)benzenesulfonamide (**13b**)*

Yield: 54 mg (59%). White solid, m.p. 179-182°C. ^{1}H NMR (400 MHz, DMSO-d_6) δ 7.70 (d, J = 8.5 Hz, 2H), 7.62 (d, J = 8.5 Hz, 2H), 7.45 – 7.31 (m, 4H), 7.23 (br.s, 2H), 5.67 (d, J = 5.3 Hz, 1H), 3.39 – 3.33 (m, 4H), 3.09 – 2.96 (m, 2H), 2.71 (dd, J = 17.0, 6.7 Hz, 1H), 1.86 – 1.68 (m, 4H) ppm. ^{13}C NMR (100 MHz, DMSO-d_6) δ 173.1, 169.5, 140.8, 140.1, 139.4, 133.0, 129.3, 129.1, 126.6, 122.5, 64.6, 46.4, 46.3, 45.0, 35.0, 25.9, 24.2 ppm. HRMS (ESI), m/z calcd for $C_{21}H_{23}ClN_3O_4S^+$ $[M+H]^+$ 448.1092, found 448.1095.

*4.2.5.3. 4-(2RS,3RS)-(2-(4-Chlorophenyl)-3-(morpholine-4-carbonyl)-5-oxopyrrolidin-1-yl)benzenesulfonamide (**13c**)*

Yield: 53 mg (56%). White solid, m.p. 167-170°C. ^{1}H NMR (400 MHz, DMSO-d_6) δ 7.70 (d, J = 8.9 Hz, 2H), 7.62 (d, J = 8.9 Hz, 2H), 7.41 – 7.35 (m, 4H), 7.23 (br.s, 2H), 5.72 (d, J = 5.3 Hz, 1H), 3.61 – 3.53 (m, 3H), 3.53 – 3.44 (m, 3H), 3.42 – 3.34 (m, 2H), 3.30 – 3.23 (m, 1H), 3.03 (dd, J = 17.0, 9.3 Hz, 1H), 2.72 (dd, J = 17.0, 6.7 Hz, 1H) ppm. ^{13}C NMR (100 MHz, DMSO) δ 172.8, 170.0, 140.7, 140.2, 139.2, 133.0, 129.3, 129.3, 126.6, 122.6, 66.4, 66.3, 64.4, 46.0, 42.7, 42.6, 35.4 ppm. HRMS (ESI), m/z calcd for $C_{21}H_{23}ClN_3O_5S^+$ $[M+H]^+$ 464.1041, found 464.1049.

*4.2.5.4. 4-(2RS,3RS)-(2-(4-Chlorophenyl)-5-oxo-3-(thiomorpholine-4-carbonyl)pyrrolidin-1-yl)benzenesulfonamide (**13d**)*

Yield: 39 mg (40%). White solid, m.p. 154-157°C. ^{1}H NMR (400 MHz, Acetone-d_6) δ 7.81 – 7.73 (m, 2H), 7.71 – 7.64 (m, 2H), 7.46 – 7.40 (m, 2H), 7.40 – 7.35 (m, 2H), 6.47 (br.s, 2H), 5.83 (d, J = 5.6 Hz, 1H), 3.95 – 3.83 (m, 2H), 3.82 – 3.70 (m, 2H), 3.66 (ddd, J = 9.3, 7.3, 5.6 Hz, 1H), 3.09 (dd, J = 17.0, 9.3 Hz, 1H), 2.79 (dd, J = 17.0, 7.3 Hz, 1H), 2.67 – 2.52 (m, 3H),

3.14 – 3.04 (m, 1H) ppm. ^{13}C NMR (100 MHz, Acetone-d_6) δ 172.1, 169.6, 141.1, 139.7, 139.2, 133.3, 129.0, 128.6, 126.5, 122.0, 64.7, 48.2, 44.8, 43.5, 35.3, 27.4, 26.9 ppm. HRMS (ESI), m/z calcd for $C_{21}H_{23}ClN_3O_4S_2^+$ $[M+H]^+$ 480.0813, found 480.0820.

*4.2.5.5. 4-((2RS,3RS)-(2-(4-Chlorophenyl)-3-(4-methylpiperazine-1-carbonyl)-5-oxopyrrolidin-1-yl)benzenesulfonamide (**13e**)*

Yield: 63 mg (65%). White solid, m.p. 161-164°C. ^{1}H NMR (400 MHz, Acetone-d_6) δ 7.84 – 7.73 (m, 2H), 7.73 – 7.65 (m, 2H), 7.43 (d, J = 8.6 Hz, 2H), 7.37 (d, J = 8.5 Hz, 2H), 6.55 (s br.s, 2H), 5.83 (d, J = 5.4 Hz, 1H), 3.84 – 3.71 (m, 1H), 3.71 – 3.57 (m, 3H), 3.56 – 3.47 (m, 1H), 3.11 (dd, J = 17.0, 9.3 Hz, 1H), 2.79 (dd, J = 17.0, 7.2 Hz, 1H), 2.66 – 2.54 (m, 3H), 2.53 – 2.44 (m, 1H), 2.39 (s, 3H) ppm. ^{13}C NMR (100 MHz, Acetone-d_6) δ 172.0, 170.0, 141.1, 139.7, 139.1, 133.4, 129.1, 128.6, 126.6, 121.9, 64.4, 52.6, 52.5, 42.3, 39.0, 34.9 ppm. HRMS (ESI), m/z calcd for $C_{22}H_{26}ClN_4O_4S^+[M+H]^+$ 477.1358, found 477.1365.

*4.2.5.6. (2RS,3RS)-2-(4-Chlorophenyl)-N-(4-methoxybenzyl)-5-oxo-1-(4-sulfamoylphenyl)pyrrolidine-3-carboxamide (**13f**)*

Yield: 63 mg (60%). White solid, m.p. 157-160°C. ^{1}H NMR (400 MHz, DMSO-d_6) δ 8.51 (t, J = 5.9 Hz, 1H), 7.75 – 7.65 (m, 2H), 7.64 – 7.56 (m, 2H), 7.37 (d, J = 8.7 Hz, 2H), 7.32 (d, J = 8.7 Hz, 2H), 7.23 (br.s, 2H), 7.16 – 7.09 (m, 2H), 6.91 – 6.85 (m, 2H), 5.59 (d, J = 6.0 Hz, 1H), 4.34 – 4.24 (m, 1H), 4.20 – 4.13 (m, 1H), 3.74 (s, 3H), 3.09 – 3.01 (m, 1H), 2.94 (dd, J = 16.9, 9.0 Hz, 1H), 2.71 (dd, J = 16.9, 7.6 Hz, 1H) ppm. ^{13}C NMR (100 MHz, Acetone-d_6) δ 172.4, 170.5, 159.0, 141.2, 139.7, 139.1, 133.2, 131.0, 128.9, 128.9, 128.6, 126.4, 122.2, 113.7, 65.1, 54.6, 47.7, 42.3, 35.1 ppm. HRMS (ESI), m/z calcd for $C_{25}H_{25}ClN_3O_5S$ [M+H]+ 514.1198, found 514.1205.

*4.2.5.7. (2RS,3RS)-2-(4-Chlorophenyl)-N-(2-(dimethylamino)ethyl)-5-oxo-1-(4-sulfamoylphenyl)pyrrolidine-3-carboxamide (**13g**)*

Yield: 40 mg (42%). White solid, m.p. 193-196°C. ^{1}H NMR (400 MHz, Acetone-d_6) δ 7.79 – 7.73 (m, 2H), 7.65 (d, J = 6.8 Hz, 2H), 7.40 (d, J = 8.7 Hz, 2H), 7.36 (d, J = 8.6 Hz, 2H), 7.24 (s, 1H), 6.47 (br.s., 2H), 5.63 (d, J = 6.2 Hz, 1H), 3.44 – 3.34 (m, 1H), 3.33 – 3.23 (m, 1H), 3.15 (ddd, J = 8.9, 8.1, 6.2 Hz, 1H), 2.94 (dd, J = 17.0, 8.9 Hz, 1H), 2.85 (dd, J = 17.0, 8.1 Hz, 1H), 2.39 (t, J = 6.3 Hz, 2H), 2.19 (s, 6H) ppm. ^{13}C NMR (100 MHz, Acetone-d_6) δ 172.5, 170.7, 141.2, 139.7, 139.3, 133.1, 128.9, 128.5, 126.4, 122.1, 65.0, 58.1, 47.4, 44.6, 37.1, 35.0 ppm. HRMS (ESI), m/z calcd for $C_{21}H_{26}ClN_4O_4S^+$ $[M+H]^+$ 465.1358, found 465.1362.

*4.2.5.8. (2RS,3RS)-2-(4-Chlorophenyl)-N-(3-(dimethylamino)propyl)-5-oxo-1-(4-sulfamoylphenyl)pyrrolidine-3-carboxamide (**13h**)*

Yield: 62 mg (64%). White solid, m.p. 190-193°C. ^{1}H NMR (400 MHz, Acetone-d_6) δ 7.77 (d, J = 8.7 Hz, 2H), 7.73 – 7.69 (m, 1H), 7.66 (d, J = 8.7 Hz, 2H), 7.41 (d, J = 8.6 Hz, 2H), 7.36 (d, J = 8.6 Hz, 2H), 6.50 (br.s, 2H), 5.65 (d, J = 6.1 Hz, 1H), 3.65 (q, J = 6.7, 6.3 Hz, 2H), 3.38 – 3.21 (m, 2H), 3.12 (ddd, J = 8.8, 8.0, 6.1 Hz, 1H), 2.94 (dd, J = 17.0, 8.8 Hz, 1H), 2.85 (dd, J = 16.9, 8.0 Hz, 1H), 2.28 (s, 6H), 1.72 (p, J = 6.7 Hz, 2H) ppm. ^{13}C NMR (100 MHz, Acetone-d_6) δ 172.5, 170.5, 141.2, 139.7, 139.3, 133.2, 128.9, 128.6, 126.4, 122.1, 65.0, 56.8, 47.7, 44.3, 37.6, 35.0, 26.5 ppm. HRMS (ESI), m/z calcd for $C_{22}H_{28}ClN_4O_4S^+$ [M+H]+ 479.1514, found 479.1521.

*4.2.5.9. 2-(2RS,3RS)-(2-(4-Chlorophenyl)-5-oxo-1-(4-sulfamoylphenyl)pyrrolidine-3-carboxamido)ethyl acetate (**13i**)*

Yield: 64 mg (66%). White solid, m.p. 195-198°C. ^{1}H NMR (400 MHz, Acetone-d_6) δ 7.81 – 7.73 (m, 2H), 7.70 – 7.62 (m, 2H), 7.54 (s, 1H), 7.40 (d, J = 8.6 Hz, 2H), 7.36 (d, J = 8.6 Hz, 2H), 6.46 (br.s, 2H), 5.64 (d, J = 6.1 Hz, 1H), 4.20 – 4.05 (m, 2H), 3.59 – 3.47 (m, 1H), 3.50 – 3.38 (m, 1H), 3.14 (ddd, J = 9.0, 8.1, 6.1 Hz, 1H), 2.95 (dd, J = 17.1, 9.0 Hz, 1H), 2.86 (dd, J = 17.1, 8.1 Hz, 1H), 1.98 (s, 3H) ppm. ^{13}C NMR (100 MHz, Acetone-d_6) δ 172.5, 171.2, 170.1, 141.2, 139.7, 139.3, 133.2, 128.9, 128.5, 126.5, 122.1, 65.0, 62.6, 47.5, 38.4, 34.9, 19.9 ppm. HRMS (ESI), m/z calcd for $C_{21}H_{23}ClN_3O_6S^+$ $[M+H]^+$ 480.0991, found 480.0991.

*4.2.5.10. 3-((2RS,3RS)-(2-(4-Chlorophenyl)-5-oxo-1-(4-sulfamoylphenyl)pyrrolidine-3-carboxamido)propyl acetate (**13j**)*

Yield: 66 mg (66%). White solid, m.p. 191-194°C. ^{1}H NMR (400 MHz, Acetone-d_6) δ 7.80 – 7.73 (m, 2H), 7.69 – 7.61 (m, 2H), 7.46 – 7.42 (m, 1H), 7.40 (d, J = 8.7 Hz, 2H), 7.35 (d, J = 8.7 Hz, 2H), 6.48 (br.s, 2H), 5.64 (d, J = 6.2 Hz, 1H), 4.13 – 3.98 (m, 2H), 3.37 (dq, J = 13.3, 6.6 Hz, 1H), 3.28 (dq, J = 13.3, 6.6 Hz, 1H), 3.12 (ddd, J = 8.9, 8.2, 6.2 Hz, 1H), 2.95 (dd, J = 17.0, 8.9 Hz, 1H), 2.86 (dd, J = 17.0, 8.2 Hz, 1H), 2.00 (s, 3H), 1.82 (p, J = 6.6 Hz, 2H) ppm. ^{13}C NMR (101 MHz, Acetone-d_6) δ 172.5, 171.0, 170.2, 141.1, 139.7, 139.2, 133.2, 129.0, 128.5, 126.4, 122.2, 65.0, 61.5, 47.7, 36.1, 35.0, 28.6, 19.9 ppm. HRMS (ESI), m/z calcd for $C_{22}H_{25}ClN_3O_6S^+$ $[M+H]^+$ 494,1147, found 494,1150.

*4.2.5.11. Methyl ((2RS,3RS)-2-(4-chlorophenyl)-5-oxo-1-(4-sulfamoylphenyl)pyrrolidine-3-carbonyl)glycinate (**13k**)*

Yield: 53 mg (54%). White solid, m.p. 190-193°C. ^{1}H NMR (400 MHz, Acetone-d_6) δ 7.87 – 7.73 (m, 3H), 7.71 – 7.60 (m, 2H), 7.43 (d, J = 8.5 Hz, 2H), 7.36 (d, J = 8.5 Hz, 2H), 6.51 (br.s, 2H), 5.67 (d, J = 5.9 Hz, 1H), 4.01 (t, J = 6.0 Hz, 2H), 3.70 (s, 3H), 3.26 (ddd, J = 9.2, 7.7, 5.9 Hz, 1H), 3.00 (dd, J = 17.2, 9.2 Hz, 1H), 2.88 (dd, J = 17.2, 7.7 Hz, 1H) ppm. ^{13}C NMR (101 MHz, Acetone-d_6) δ 172.4, 171.7, 169.9, 141.1, 139.7, 139.1, 133.2, 128.9, 128.6, 126.5, 122.1, 64.9, 51.4, 47.0, 40.9, 34.9 ppm. HRMS (ESI), m/z calcd for $C_{20}H_{21}ClN_3O_6S^+$ $[M+H]^+$ 466.0834, found 466.0839.

*4.2.5.12. Methyl 3-((2RS,3RS)-2-(4-chlorophenyl)-5-oxo-1-(4-sulfamoylphenyl)pyrrolidine-3-carboxamido)propanoate (**13l**)*

Yield: 53 mg (54%). White solid, m.p. 201-204°C. ^{1}H NMR (400 MHz, Acetone-d_6) δ 7.80 – 7.71 (m, 2H), 7.69 – 7.61 (m, 2H), 7.45 (s, 1H), 7.39 (d, J = 8.8 Hz, 2H), 7.35 (d, J = 8.8 Hz, 2H), 6.46 (br.s, 2H), 5.62 (d, J = 6.1 Hz, 1H), 3.63 (s, 3H), 3.57 – 3.49 (m, 1H), 3.48 – 3.40 (m, 1H), 3.13 (ddd, J = 8.9, 8.0, 6.1 Hz, 1H), 2.94 (dd, J = 17.0, 8.9 Hz, 1H), 2.85 (dd, J = 17.0, 8.0 Hz, 1H), 2.55 (t, J = 6.6 Hz, 2H) ppm. ^{13}C NMR (100 MHz, Acetone-d_6) δ 172.5, 171.7, 170.9, 141.1, 139.6, 139.2, 133.2, 128.9, 128.5, 126.5, 122.1, 65.0, 50.9, 47.4, 35.2, 34.9, 33.6 ppm. HRMS (ESI), m/z calcd for $C_{21}H_{23}ClN_3O_6S^+$ $[M+H]^+$ 480.0991, found 480.0995.

*4.2.5.13. Methyl 4-((2RS,3RS)-2-(4-chlorophenyl)-5-oxo-1-(4-sulfamoylphenyl)pyrrolidine-3-carboxamido)butanoate (**13m**)*

Yield: 49 mg (49%). White solid, m.p. 197-200°C. ^{1}H NMR (400 MHz, Acetone-d_6) δ 7.82 – 7.73 (m, 2H), 7.69 – 7.61 (m, 2H), 7.43 (t, J = 5.9 Hz, 1H), 7.39 (d, J = 8.7 Hz, 2H), 7.35 (d, J = 8.7 Hz, 2H), 6.49 (br.s, 2H), 5.64 (d, J = 6.3 Hz, 1H), 3.63 (s, 3H), 3.37 – 3.27 (m, 1H), 3.29 – 3.16 (m, 1H), 3.12 (ddd, J = 8.9, 8.2, 6.3 Hz, 1H), 2.94 (dd, J = 17.0, 8.8 Hz, 1H), 2.86 (dd, J = 17.0, 8.2 Hz, 1H), 2.32 (t, J = 7.4 Hz, 2H), 1.78 (p, J = 7.4 Hz, 2H) ppm. ^{13}C NMR (100 MHz, Acetone-d_6) δ 172.9, 172.6, 170.9, 141.1, 139.7, 139.2, 133.2, 128.9, 128.5, 126.4, 122.2, 65.1, 50.8, 47.8, 38.6, 35.1, 30.7, 24.7 ppm. HRMS (ESI), m/z calcd for $C_{22}H_{25}ClN_3O_6S^+$ $[M+H]^+$ 494,1147, found 494,1151.

*4.2.5.14. (2RS,3RS)-2-(4-Chlorophenyl)-N-(2-morpholinoethyl)-5-oxo-1-(4-sulfamoylphenyl)pyrrolidine-3-carboxamide (**13n**)*

Yield: 66 mg (64%). White solid, m.p. 177-180°C. ^{1}H NMR (400 MHz, Acetone-d_6) δ 8.46 (t, J = 5.6 Hz, 1H), 7.82 – 7.74 (m, 2H), 7.70 – 7.62 (m, 2H), 7.40 (d, J = 8.6 Hz, 2H), 7.35 (d, J = 8.5 Hz, 2H), 6.50 (br.s, 2H), 5.68 (d, J = 5.4 Hz, 1H), 4.13 – 3.77 (m, 5H), 3.76 – 3.54 (m, 3H), 3.52 – 3.39 (m, 2H), 3.25 (s, 2H), 3.17 (ddd, J = 9.0, 7.0, 5.4 Hz, 1H), 2.97 (dd, J = 17.1, 9.0 Hz,

1H), 2.83 (dd, *J* = 17.1, 7.0 Hz, 1H) ppm.^{13}C NMR (100 MHz, Acetone-d_6) δ 172.5, 171.9, 141.2, 139.57, 139.0, 133.2, 129.0, 128.4, 126.5, 121.8, 64.69, 63.4, 56.6, 52.0, 47.1, 34.8, 33.6 ppm. HRMS (ESI), m/z calcd for $C_{23}H_{28}ClN_4O_5S^+$ $[M+H]^+$ 507.1463, found 507.1470.

*4.2.5.15. (2RS,3RS)-2-(4-Chlorophenyl)-N-(3-morpholinopropyl)-5-oxo-1-(4-sulfamoylphenyl)pyrrolidine-3-carboxamide (**13o**)*

Yield: 61 mg (58%). White solid, m.p. 148-151°C. ^{1}H NMR (400 MHz, Acetone-d_6) δ 7.76 (d, J = 8.8 Hz, 2H), 7.68 – 7.60 (m, 2H), 7.53 (t, J = 5.3 Hz, 1H), 7.40 (d, J = 8.7 Hz, 2H), 7.36 (d, J = 8.7 Hz, 2H), 6.47 (br.s, 2H), 5.62 (d, J = 6.5 Hz, 1H), 3.73 – 3.45 (m, 4H), 3.34 (dq, J = 12.8, 6.4 Hz, 1H), 3.26 (dq, J = 13.2, 6.4 Hz, 1H), 3.13 – 3.04 (m, 1H), 2.98 – 2.89 (m, 1H), 2.87 – 2.79 (m, 1H), 2.39 – 2.27 (m, 6H), 1.65 (p, J = 6.8 Hz, 2H) ppm. ^{13}C NMR (100 MHz, Acetone-d_6) δ 172.6, 170.7, 141.1, 139.8, 139.2, 133.2, 129.0, 128.6, 126.4, 122.3, 66.5, 65.1, 56.4, 56.4, 53.6, 47.99, 47.9, 38.1, 35.1, 25.7 ppm. HRMS (ESI), m/z calcd for $C_{24}H_{30}ClN_4O_5S$ [M+H]+ 521.1620, found 521.1628.

*4.2.5.16. (2RS,3RS)-2-(4-Chlorophenyl)-5-oxo-N-(3-(pyrrolidin-1-yl)propyl)-1-(4-sulfamoylphenyl)pyrrolidine-3-carboxamide (**13p**)*

Yield: 61 mg (60%). White solid, m.p. 161-164°C. ^{1}H NMR (400 MHz, Acetone-d_6) δ 7.80 – 7.73 (m, 2H), 7.70 – 7.59 (m, 3H), 7.40 (d, *J* = 8.8 Hz, 2H), 7.36 (d, *J* = 8.8 Hz, 2H), 6.51 (br.s, 2H), 5.62 (d, *J* = 6.4 Hz, 1H), 3.34 (ddd, *J* = 13.6, 12.2, 6.4 Hz, 1H), 3.26 (ddd, *J* = 13.3, 6.7, 5.1 Hz, 1H), 3.07 (ddd, *J* = 8.6, 8.5, 6.4 Hz, 1H), 2.92 (dd, *J* = 16.9, 8.6 Hz, 1H), 2.86 (dd, *J* = 16.9, 8.5 Hz, 1H), 2.55 – 2.29 (m, 6H), 1.79 – 1.52 (m, 6H) ppm. ^{13}C NMR (100 MHz, Acetone-d_6) δ 172.5, 170.4, 170.3, 141.1, 139.7, 139.3, 133.2, 128.9, 128.5, 126.4, 122.2, 65.1, 54.0, 53.7, 48.0, 38.3, 35.0, 27.9, 23.2 ppm. HRMS (ESI), m/z calcd for $C_{24}H_{30}ClN_4O_4S^+$ $[M+H]^+$ 505.1671, found 505.1676.

*4.2.5.17. (2RS,3RS)-N-(3-(1H-Imidazol-1-yl)propyl)-2-(4-chlorophenyl)-5-oxo-1-(4-sulfamoylphenyl)pyrrolidine-3-carboxamide (**13q**)*

Yield: 64 mg (63%). White solid, m.p. 167-170°C. ^{1}H NMR (400 MHz, Acetone-d_6) δ 9.06 (s, 1H), 7.85 (t, *J* = 6.0 Hz, 1H), 7.81 – 7.73 (m, 3H), 7.69 – 7.62 (m, 3H), 7.41 (d, *J* = 8.6 Hz, 2H), 7.35 (d, *J* = 8.6 Hz, 2H), 6.57 (br.s, 2H), 5.69 (d, *J* = 5.9 Hz, 1H), 4.43 (t, *J* = 6.8 Hz, 2H), 3.39 – 3.28 (m, 2H), 3.19 (ddd, *J* = 9.0, 7.6, 5.9 Hz, 1H), 3.00 (dd, *J* = 17.0, 9.0 Hz, 1H), 2.87 (dd, *J* = 17.0, 7.6 Hz, 1H), 2.18 (p, *J* = 6.7 Hz, 2H) ppm. ^{13}C NMR (100 MHz, Acetone-d_6) δ 172.7, 171.8, 141.1, 139.6, 139.1, 135.6, 133.3, 129.0, 128.6, 126.5, 122.1, 122.0, 120.2, 64.9, 47.4,

46.8, 35.7, 35.1, 30.2 ppm. HRMS (ESI), m/z calcd for $C_{23}H_{25}ClN_5O_4S^+$ $[M+H]^+$ 502.1310, found 502.1318.

*4.2.5.18. (2RS,3RS)-2-(4-Chlorophenyl)-N-(3-(4-methylpiperazin-1-yl)propyl)-5-oxo-1-(4-sulfamoylphenyl)pyrrolidine-3-carboxamide (**13r**)*

Yield: 63 mg (58%). White solid, m.p. 178-181°C. ^{1}H NMR (400 MHz, Acetone-d_6) δ 7.79 – 7.74 (m, 2H), 7.67 – 7.63 (m, 2H), 7.63 – 7.56 (m, 1H), 7.40 (d, J = 8.7 Hz, 2H), 7.37 (d, J = 8.7 Hz, 2H), 6.48 (br. s, 2H), 5.62 (d, J = 6.3 Hz, 1H), 3.34 (dq, J = 12.7, 6.3 Hz, 1H), 3.26 (qd, J = 6.8, 5.2 Hz, 1H), 3.13 – 2.82 (m, 7H), 2.43 – 2.34 (m, 6H), 2.24 (s, 3H), 1.67 (p, J = 6.8 Hz, 2H) ppm. ^{13}C NMR (100 MHz, Acetone-d_6) δ 172.7, 171.6, 141.1, 139.7, 139.1, 133.2, 129.0, 128.6, 126.5, 122.1, 65.0, 54.1, 49.9, 48.4, 47.4, 42.8, 36.2, 34.9, 23.9 ppm. HRMS (ESI), m/z calcd for $C_{25}H_{33}ClN_5O_4S^+$ [M+H]+ 534,1936, found 534,1942.

*4.2.6. Synthesis of **13s,t***

4.2.6. Precursor **13i,j** (0.06 mmol) was dissolved in methanol (3 mL) and solution of $LiOHxH_2O$ (8 mg, 0.18 mmol) in H_2O (1 mL) was added. The mixture was stirred at 50°C for 5 hours and the reaction course was monitored by TLC. After the reaction completion 10% aqueous solution of HCl was added to neutralize pH of the mixture. Methanol was removed in vacuo and the residue was dissolved in ethyl acetate (3 mL), washed with H_2O (3x1 mL) and brine (1 mL), dried over Na_2SO_4, filtered and concentrated to give **13s,t** (**ASA11,13)** in high yields.

*4.2.6.1. (2RS,3RS)-2-(4-Chlorophenyl)-N-(2-hydroxyethyl)-5-oxo-1-(4-sulfamoylphenyl)pyrrolidine-3-carboxamide (**13s**)*

Yield: 23 mg (88%). White solid, m.p. 155-158°C. ^{1}H NMR (400 MHz, DMSO-d_6) δ 8.10 (t, J = 5.6 Hz, 1H), 7.69 (d, J = 8.9 Hz, 2H), 7.61 (d, J = 8.9 Hz, 2H), 7.37 (d, J = 8.6 Hz, 2H), 7.32 (d, J = 8.6 Hz, 2H), 7.23 (br.s, 2H), 5.57 (d, J = 5.3 Hz, 1H), 4.66 (br.s, 1H), 3.40 (dp, J = 9.4, 5.0 Hz, 2H), 3.16 (q, J = 5.8 Hz, 2H), δ 3.03 – 2.97 (m, 1H), 2.93 (dd, J = 16.5, 9.2 Hz, 1H), 2.67 (dd, J = 16.5, 6.5 Hz, 1H) ppm. ^{13}C NMR (100 MHz, Acetone-d_6) δ 172.7, 171.1, 140.4, 139.7, 139.0, 132.4, 128.8, 128.6, 126.1, 122.1, 64.4, 59.7, 46.2, 41.7, 35.1 ppm. HRMS (ESI), m/z calcd for $C_{19}H_{21}ClN_3O_5S^+$ $[M+H]^+$ 438.0885, found 438.0891.

*4.2.6.2. (2RS,3RS)-2-(4-Chlorophenyl)-N-(3-hydroxypropyl)-5-oxo-1-(4-sulfamoylphenyl)pyrrolidine-3-carboxamide (**13t**)*

Yield: 22 mg (81%). White solid, m.p. 157-160°C. ^{1}H NMR (400 MHz, Acetone-d_6) δ 7.80 – 7.73 (m, 2H), 7.68 – 7.63 (m, 2H), 7.49 – 7.42 (m, 1H), 7.40 (d, J = 8.7 Hz, 2H), 7.36 (d, J = 8.7 Hz, 2H), 6.49 (br.s, 2H), 5.65 (d, J = 6.3 Hz, 1H), 3.55 (t, J = 6.1 Hz, 2H), 3.40 – 3.28 (m, 3H), 3.20 – 3.07 (m, 1H), 2.95 (dd, J = 17.0, 8.9 Hz, 1H), 2.86 (dd, J = 17.0, 8.2 Hz, 1H), 1.66 (p, J = 6.4 Hz, 2H) ppm. ^{13}C NMR (101 MHz, Acetone-d_6) δ 172.7, 171.3, 141.1, 139.7, 139.1, 133.2, 129.0, 128.6, 126.5, 122.3, 65.1, 58.8, 47.6, 36.3, 35.1, 32.3 ppm. HRMS (ESI), m/z calcd for $C_{20}H_{23}ClN_3O_5S^+$ $[M+H]^+$ 452.1041, found 452.1045.

*4.2.7. Synthesis of **13u-w***

Precursor **13k-m** (0.09 mmol) was dissolved in methanol (3 mL) and solution of $LiOH{\cdot}H_2O$ (8 mg, 0.18 mmol) in H_2O (1 mL) was added. The mixture was stirred at 50°C overnight and the reaction course was monitored by TLC. After the reaction completion 10% aqueous solution of HCl was added to decrease pH of the mixture to 3. Methanol was removed in vacuo and the residue was dissolved in ethyl acetate (3 mL), washed with H_2O (3x1 mL) and brine (1 mL), dried over Na_2SO_4, filtered and concentrated to give **13u-w** in high yields.

*4.2.7.1. ((2RS,3RS)-2-(4-Chlorophenyl)-5-oxo-1-(4-sulfamoylphenyl)pyrrolidine-3-carbonyl)glycine (**13u**)*

Yield: 29 mg (73%). White solid, m.p. 202-205°C. ^{1}H NMR (400 MHz, Acetone-d_6) δ 10.94 (s, 1H), δ 7.80 – 7.76 (m, 2H), 7.73 (t, J = 5.8 Hz, 1H), 7.69 – 7.64 (m, 2H), 7.47 – 7.39 (m, 2H), 7.38 – 7.31 (m, 2H), 6.50 (br.s, 2H), 5.69 (d, J = 5.8 Hz, 1H), 4.01 (dd, J = 5.8, 3.0 Hz, 2H), 3.28 (ddd, J = 9.1, 7.6, 5.9 Hz, 1H), 3.01 (dd, J = 17.1, 9.1 Hz, 1H), 2.89 (dd, J = 17.1, 7.6 Hz, 1H) ppm. ^{13}C NMR (100 MHz, Acetone-d_6) δ 172.4, 171.5, 170.1, 141.2, 139.7, 139.2, 133.2, 128.9, 128.6, 126.5, 122.0, 64.9, 46.9, 40.6, 34.8 ppm. HRMS (ESI), m/z calcd for $C_{19}H_{19}ClN_3O_6S^+$ $[M+H]^+$ 452.0678, found 452.0677.

*4.2.7.2. 3-((2RS,3RS)-2-(4-Chlorophenyl)-5-oxo-1-(4-sulfamoylphenyl)pyrrolidine-3-carboxamido)propanoic acid (**13v**)*

Yield: 34 mg (81%). White solid, m.p. 205-208°C. ^{1}H NMR (400 MHz, Acetone-d_6) δ 10.81 (br. s, 1H), 7.80 – 7.75 (m, 2H), 7.68 – 7.63 (m, 2H), 7.51 (t, J = 5.8 Hz, 1H), 7.38 (d, J = 8.7 Hz, 2H), 7.34 (d, J = 8.7 Hz, 2H), 6.49 (br.s, 2H), 5.65 (d, J = 6.1 Hz, 1H), 3.58 – 3.48 (m, 1H), 3.51 – 3.38 (m, 1H), 3.16 (ddd, J = 8.9, 8.1, 6.1 Hz, 1H), 2.95 (dd, J = 17.1, 8.9 Hz, 1H), 2.87 (dd, J = 17.1, 8.1 Hz, 1H), 2.56 (t, J = 6.6 Hz, 2H) ppm. ^{13}C NMR (100 MHz, Acetone-d_6) δ 172.6, 172.3, 171.1, 141.1, 139.7, 139.2, 133.2, 128.9, 128.5, 126.5, 122.2, 65.0, 47.3, 35.4, 34.9, 33.4 ppm. HRMS (ESI), m/z calcd for $C_{20}H_{21}ClN_3O_6S^+$ $[M+H]^+$ 466,0834, found 466,0840.

*4.2.7.3. 4-((2RS,3RS)-2-(4-Chlorophenyl)-5-oxo-1-(4-sulfamoylphenyl)pyrrolidine-3-carboxamido)butanoic acid (**13w**)*

Yield: 38 mg (87%). White solid, m.p. 220-223°C. ^{1}H NMR (400 MHz, Acetone-d_6) δ 10.92 (br.s, 1H), 7.80 – 7.75 (m, 2H), 7.68 – 7.61 (m, 2H), 7.47 (t, J = 5.9 Hz, 1H), 7.40 (d, J = 8.6 Hz, 2H), 7.35 (d, J = 8.6 Hz, 2H), 6.48 (br.s, 2H), 5.65 (d, J = 6.3 Hz, 1H), 3.38 – 3.29 (m, 1H), 3.28 – 3.20 (m, 1H), 3.13 (ddd, J = 8.5, 8.2, 6.3 Hz, 1H), 2.95 (dd, J = 17.0, 8.8 Hz, 1H), 2.87 (dd, J = 17.0, 8.2 Hz, 1H), 2.32 (t, J = 7.4 Hz, 2H), 1.78 (p, J = 7.1 Hz, 2H) ppm. ^{13}C NMR (101 MHz, Acetone-d_6) δ 173.5 172.6, 170.9, 141.1, 139.6, 139.2, 133.2, 128.9, 128.5, 126.5, 122.2, 65.0, 47.7, 38.5, 35.0, 30.6, 24.7 ppm. HRMS (ESI), m/z calcd for $C_{21}H_{23}ClN_3O_6S^+$ $[M+H]^+$ 480.0991, found 480.0996.

4.3. Carbonic anhydrase inhibition assay

An Applied Photophysics stopped-flow instrument has been used for assaying the CA catalyzed CO_2 hydration activity [44]. Phenol red (at a concentration of 0.2 mM) has been used as indicator, working at the absorbance maximum of 557 nm, with 20 mM Tris (pH 8.3) as buffer, and 20 mM Na_2SO_4 (for maintaining constant the ionic strength), following the initial rates of the CA-catalyzed CO_2 hydration reaction for a period of 10–100 s. The CO_2 concentrations ranged from 1.7 to 17 mM for the determination of the kinetic parameters and inhibition constants. For each inhibitor at least six traces of the initial 5–10% of the reaction have been used for determining the initial velocity. The uncatalyzed rates were determined in the same manner and subtracted from the total observed rates. Stock solutions of inhibitor (0.1 mM) were prepared in distilled-deionized water and dilutions up to 0.005 nM were done thereafter with the assay buffer. Inhibitor and enzyme solutions were preincubated together for 15 min at room temperature prior to assay, in order to allow for the formation of the E-I complex. The inhibition constants were obtained by non-linear least-squares methods using PRISM 3 and the Cheng-Prusoff equation, as reported earlier, and represent the mean from at least three different determinations. All CA isoforms were recombinant ones obtained in-house [63-66].

4.4. Cell culture

Retinal pigment epithelial cells ARPE-19 were obtained from American Type Culture Collection (ATCC, Manassas, VA, USA). T98G cells derived from a human glioblastoma multiforma tumor were obtained from Russian Cell Culture Collection (Institute of Cytology RAS). Cell lines were grown in Dulbeccos Modified Eagle's Medium-F12 (BioloT) containing 10% (v/v) heat-inactivated fetal calf serum (FCS, HyClone Laboratories, UT, USA), 1% L-glutamine, 1%

sodium pyruvate, 50 U/mL penicillin, and 50 μg/mL streptomycin (BioloT) in a humidified atmosphere containing 95% air and 5% CO_2, at 37 ◦ C.

4.5. Cell viability assay

Cytotoxicity of carbonic anhydrase inhibitors was tested using colorimetric assay with tetrazolium dye – 3-(4,5-dimethylthiazol-2-yl)-2,5-diphenyltetrazolium bromide (MTT). The cell lines were cultured for 48 h under normoxia and in the presence of the hypoxia-mimicking agent 50 μM $CoCl_2$ with medium containing different concentrations of test compounds. Following treatment, Dulbeccos Modified Eagle's Medium-F12 (100 μL/ well) and 20 μL of a 2.5 mg/mL MTT reagent were added and cells were maintained for 1 h at 37 °C. The amount of cells was 5 × 10^3 cells/200 μL/well in 96-well plates. After aspiration of the supernatants, the MTT-formazan crystals formed by metabolically active cells were dissolved in dimethyl sulfoxide (100 μL/well) and absorbance was acquired at 540 nm and 690 nm in Varioskan LUX™ Multimode Microplate Reader (Thermo Scientific, USA). Values measured at 540 nm were subtracted for background correction at 690 nm, and the data were presented as a percent of control untreated samples.

4.6. Total RNA isolation, reverse transcription and quantitative real-time PCR

Total RNA was isolated and purified from T98G cells using Biosilica RNA extraction kit (Biosilica, Novosibirsk, Russia) according to manufacturer's protocol. RNA concentration was evaluated by the absorbance at 260 nm using a NanoDrop 2000c Spectrophotometer (Thermo Scientific, USA). The ratio of absorbance at 260 nm and 280 nm for pure RNA preparations was in the range of >1.8 and < 2.2 [Sambrook, J., Fritsch, E.F., Maniatis, T., 1989. Molecular Cloning: A Laboratory Manual, second ed. Cold Spring Harbor Laboratory Press, NY.]. The integrity of total RNA and DNA contamination were assessed by native 1% agarose gel electrophoresis [Sambrook, J., Russel, D.W., 2001. Molecular Cloning: A Laboratory Manual. CSH Laboratory Press, Cold Spring Harbor, NY]. Intact 28S and 18S rRNA were appeared on an agarose gel as sharp bands with intensity ratio ~ 2:1 and no signs of genomic DNA contaminations were observed. Equal amounts of total RNA were reverse transcribed using MMLV RT First-Strand cDNA synthesis kit (Evrogen, Moscow, Russia) in reactions containing 150 ng of total RNA. The reaction mixture (25 μl), with 15 ng cDNA, 5 μl of qPCRmix-HS SYBR mastermix (Evrogen, Moscow, Russia), 0,2 μM of forward and reverse primers, and water, was run in a LightCycler® 96 Instrument (Roche Life Science, Switzerland). The quantitative real-time PCR was performed as follows: 95 °C for 2 min, 35 cycles of 95 °C for 30s, 55 °C for 30s and 72 °C for 45s. The amount of *h*CA IV mRNA was calculated relative to

the amount of housekeeping gene GAPDH (glyceraldehyde 3-phosphate dehydrogenase) mRNA in the same sample by the equation $X_0/R_0 = 2C_tR-C_tX$, where X_0 is the original amount of *h*CA IV mRNA, R0 is the original amount of GAPDH mRNA, C_tR is the C_t (cycle threshold) value for GAPDH, and C_tX is the C_t value for *h*CA IV. The following primers for PCR analysis were purchased from Evrogen (Moscow, Russia): *h*CA IV forward primer (5'-CGATGAGAAGGTCGTCTGGACT-3'), *h*CA IV reverse primer (5'-GCCTGACATTGTCCTTCATGCTC-3') and GAPDH forward primer (5'-GTCTCCTCTGACTTCAACAGCG-3'), GAPDH reverse primer (5'-ACCACCCTGTTGCTGTAGCCAA-3'). Primers span an exon-exon junction to reduce the risk of false positives from amplification of any contaminating genomic DNA.

4.5. Docking studies

Crystal structures of *h*CA IV (5JN8) was used in docking computation. Input 3D ligand structures were prepared by LigPrep (LigPrep, version 3.3, Schrödinger, LLC, New York, NY, 2015) and Epik (Epik, version 3.1, Schrödinger, LLC, New York, NY, 2015) for the evaluation of their ionization states. The target structures were prepared according to the recommended Protein Preparation module in Maestro - Schrödinger suite [Maestro, version 10.1, Schrödinger, LLC, New York, NY, 2015], assigning bond orders, adding hydrogens, deleting water molecules, and optimizing H-bonding networks. Finally, energy minimization with a root-mean-square deviation (rmsd) value of 0.30 was applied using an Optimized Potentials for Liquid Simulation (OPLS_2005, Schrödinger, New York, NY, USA) force field. Docking experiments were carried out with Glide standard precision (SP) (Glide, version 6.6, Schrödinger, LLC, New York, NY, 2015) using grids prepared with default settings and centered in the centroid of the complexed ligand. All computations were performed on an Intel 2xCPU Xeon 6-core E5-2620 v2 @ 2.10 GHz (1200 MHz) 15MB processor running Linux.

Acknowledgements

This research was supported by the Russian Federation Government Megagrant 14.W03.031.0025. We are grateful to the Centre for Chemical Analysis and Materials Research of Saint Petersburg State University Research Park for the high-resolution mass-spectrometry data.

A. Supplementary material

Supplementary data associated with this article can be found, in the online version, at http://dx.doi.org/xxx.

References

[1] C. T. Supuran, Structure and function of carbonic anhydrases, Biochem. J. 473 (2016) 2023–2032.

[2] V. Alterio, A. Di Fiore, K. D'Ambrosio, C.T. Supuran, G. De Simone, Multiple Binding Modes of Inhibitors to Carbonic Anhydrases: How to Design Specific Drugs Targeting 15 Different Isoforms?, Chem. Rev. 112 (2012) 4421-4468.

[3] C.T. Supuran, Carbonic anhydrase inhibitors and activators for novel therapeutic applications, Future Med. Chem. 3 (2011) 1165-1180.

[4] C.T. Supuran, Diuretics: from classical carbonic anhydrase inhibitors to novel applications of the sulfonamides, Curr. Pharm. Des. 14 (2008) 641−648.

[5] C.T. Supuran, A. Scozzafava, F. Mincione, The development of topically acting carbonic anhydrase inhibitors as antiglaucoma agents, Curr. Pharm. Des. 14 (2008) 649−654.

[6] A. Scozzafava, C. T. Supuran, Glaucoma and the applications of carbonic anhydrase inhibitors, Subcell. Biochem. 75 (2014) 349-359.

[7] J.P. Hughes, S. Rees, S.B. Kalindjian, K.L. Philpott, Principles of early drug discovery, Br. J. Pharmacol. 162 (2011) 1239–1249.

[8] M. Krasavin, M. Korsakov, Z. Zvonaryova, E. Semyonychev, T. Tuccinardi, S. Kalinin, M. Tanç, C.T. Supuran, Human carbonic anhydrase inhibitory profile of mono- and bis-sulfonamides synthesized via a direct sulfochlorination of 3-and 4-(hetero)arylisoxazol-5-amine scaffolds, Bioorg. Med. Chem. 25 (2017) 1914-1925.

[9] C.T. Supuran, S. Kalinin, M. Tanç, P. Sarnpitak, P. Mujumdar, S.-A. Poulsen, M. Krasavin, Isoform-selective inhibitory profile of 2-imidazoline-substituted benzenesulfonamides against a panel of human carbonic anhydrases, J. Enzyme Inhib. Med. Chem. 31 (2016) 197-202.

[10] G. La Regina, A. Coluccia, V. Famiglini, S. Pelliccia, L. Monti, D. Vullo, E. Nuti, V. Alterio, G. De Simone, S. M. Monti, P. Pan, S. Parkkila, C.T. Supuran, A. Rossello, R. Silvestri, Discovery of 1,1′-Biphenyl-4-sulfonamides as a New Class of Potent and Selective Carbonic Anhydrase XIV Inhibitors, J. Med. Chem. 58 (2015) 8564-8572.

[11] J. Ivanova, F. Carta, D. Vullo, J. Leitans, A. Kazaks, K. Tars, R. Žalubovskis, C.T. Supuran, N-Substituted and ring opened saccharin derivatives selectively inhibit transmembrane, tumor-associated carbonic anhydrases IX and XII, Bioorg. Med. Chem. 25 (2017) 3583-3589.

[12] F. Carta, D. Vullo, S. M. Osman, Z. Al-Othman, C. T. Supuran, Synthesis and Carbonic Anhydrase inhibition of a series of SLC-0111 analogs, Bioorg. Med. Chem. 25 (2017) 2569–2576.

[13] Phase II study for metastatic pancreatic ductal adenocarcinoma in combination with gemcitabine anticancer drug is scheduled to be completed in May 2022, according to: US National Institutes of Health, US National Library of Medicine. https://www.clinicaltrials.gov/ct2/show/NCT03450018?term=SLC-0111&rank=1, 2019 (accessed 27 July 2019).

[14] C.T. Supuran, Carbonic anhydrases: novel therapeutic applications for inhibitors and activators, Nat. Rev. Drug Disc. 7 (2008) 168-181.

[15] B. W. Clare, C.T. Supuran, A perspective on quantitative structure-activity relationships and carbonic anhydrase inhibitors, Expert Opin. Drug Metab. Toxicol. 2 (2006) 113-137.

[16] C.-K. Tong, L. P. Brion, C. Suarez, M. Chesler, Interstitial Carbonic Anhydrase (CA) Activity in Brain Is Attributable to Membrane-Bound CA Type IV, J. Neurosci. 20 (2000) 8247-8253.

[17] A. Verkhratsky, A. M. Butt, Numbers: how many glial cells are in the brain?, in: A. Verkhratsky, A. M. Butt (Eds.), Glial Physiology and Pathophysiology, John Wiley and Sons, 2013, pp. 93–96.

[18] N. Svichar, M. Chesler, Surface Carbonic Anhydrase Activity on Astrocytes and Neurons Facilitates Lactate Transport, Glia 41 (2003) 415-419.

[19] N. Svichar, S. Esquenazi, A. Waheed, W. S. Sly, M. Chesler, Functional Demonstration of Surface Carbonic Anhydrase IV Activity on Rat Astrocytes, Glia 53 (2006) 241-247.

[20] M. H. Stridh, M. D. Alt, S. Wittmann, H. Heidtmann, M. Aggarwal, B. Riederer, U. Seidler, G. Wennemuth, R. McKenna, J. W Deitmer, H. M. Becker, Lactate flux in astrocytes is enhanced by a non-catalytic action of carbonic anhydrase II, J. Physiol. 590 (2012) 2333–2351.

[21] L. S. Forero-Quintero, S. Ames, H.-P. Schneider, A. Thyssen, C. D. Boone, J. T. Andring, R. McKenna, J. R. Casey, J. W. Deitmer, H. M. Becker, Membrane-anchored carbonic anhydrase IV interacts with monocarboxylate transporters *via* their chaperones CD147 and GP70, J. Biol. Chem. 294 (2019) 593–607.

[22] S. Ferrari, E. Di Iorio, V. Barbaro, D. Ponzin, F.S. Sorrentino, F. Parmeggiani, Retinitis pigmentosa: genes and disease mechanisms, Curr. Genomics 12 (2011) 238–249.

[23] A. Waheed, W. S. Sly, Carbonic anhydrase IV, in: C. T. Supuran and G. De Simone (Eds.), Carbonic Anhydrases as Biocatalysts, Elsevier, 2015, pp. 109-124.

[24] Singh, S., Lomelino, C.L., Mboge, M. Y., Frost, S. C., McKenna, R., 2018. Cancer Drug Development of Carbonic Anhydrase Inhibitors beyond the Active Site. Molecules. 23 (05), e1045.

[25] A. Sapegin, S. Kalinin, A. Angeli, C.T. Supuran, M. Krasavin, Unprotected primary sulfonamide group facilitates ring-forming cascade en route to polycyclic [1.4]oxazepine-based carbonic anhydrase inhibitors, Bioorg. Chem. 76 (2018) 140-146.

[26] M. Krasavin, M. Korsakov, O. Ronzhina, T. Tuccinardi, S. Kalinin, M. Tanç, C.T. Supuran, Primary mono- and bis-sulfonamides obtained via regiospecific sulfochlorination of N-arylpyrazoles: inhibition profile against a panel of human carbonic anhydrases, J. Enzyme Inhib. Med. Chem. 32 (2017) 920-934.

[27] L. Vats, V. Sharma, A. Angeli, R. Kumar, C. T. Supuran, P. K. Sharma, Synthesis of novel 4-functionalized 1,5-diaryl-1,2,3-triazoles containing benzenesulfonamide moiety as carbonic anhydrase I, II, IV and IX inhibitors, Eur. J. Med. Chem. 150 (2018) 678-686.

[28] S. Angapelly, P. V. Ramya, A. Angeli, S. M. Monti, M. Buonanno, M. Alvala, C. T. Supuran, M. Arifuddin, Discovery of 4-sulfamoyl-phenyl-β-lactams as a new class of potent carbonic anhydrase isoforms I, II, IV and VII inhibitors: The first example of subnanomolar CA IV inhibitors, Bioorg. Med. Chem. 25 (2017) 539-544.

[29] C. D. Boone, M. Pinard, R. McKenna, D. Silverman, Catalytic mechanism of α-class carbonic anhydrases: CO_2 hydration and proton transfer, Sub-cell. Biochem. 75 (2014) 31–52.

[30] M. K. Buemi, A. Di Fiore, L. De Luca, A. Angeli, F. Mancuso, S. Ferro, S. M. Monti, M. Buonanno, E. Russo, G. De Sarro, G. De Simone, C. T. Supuran, R. Gitto, Exploring structural properties of potent human carbonic anhydrase inhibitors bearing a 4-(cycloalkylamino-1-carbonyl)benzenesulfonamide moiety, Eur. J. Med. Chem. 163 (2019) 443-452.

[31] J. J. Baldwin, G. S Ponticello, P. S. Anderson, M.E. Christy, M. A. Murcko, W.C. Randall, H. Schwam, M. F. Sugrue, P. Gautheron, Thienothiopyran-2-sulfonamides: novel topically active carbonic anhydrase inhibitors for the treatment of glaucoma, J. Med. Chem. 32 (1989), 2510–2513.

[32] R. E. Babine, S. L. Bender, Molecular Recognition of Protein−Ligand Complexes: Applications to Drug Design, Chem. Rev. 97 (1997) 1359–1472.

[33] A. Thiry, M. Ledecq, A. Cecchi, J.-M. Dogné, J. Wouters, C. T. Supuran, & B. Masereel, Indanesulfonamides as Carbonic Anhydrase Inhibitors. Toward Structure-Based Design of Selective Inhibitors of the Tumor-Associated Isozyme CA IX, J. Med. Chem. 49 (2006) 2743–2749.

[34] A. Thiry, M. Ledecq, A. Cecchi, R. Frederick, J.-M. Dogné, C. T. Supuran, J. Wouters, B. Masereel, Ligand-based and structure-based virtual screening to identify carbonic anhydrase IX inhibitors, Bioorg. Med. Chem. 17 (2009) 553-557.

[35] O. Guzela, A. Innocenti, D. Vullo, A. Scozzafava & C. T. Supuran, 3-Phenyl-1H-Indole-5-Sulfonamides: Structure-Based Drug Design of a Promising Class of Carbonic Anhydrase Inhibitors, Cur. Pharm. Des. 16 (2010) 3317–3326.

[36] S. Gluszok, R. Frédérick, C. Foulon, F. Klupsch, C.T. Supuran, D. Vullo, A. Scozzafava, J.-F. Goossens, B. Masereel, P. Depreux, L. Goossens, Chemistry Design, solid-phase synthesis, and biological evaluation of novel 1,5-diarylpyrrole-3-carboxamides as carbonic anhydrase IX inhibitors, Bioorg. Med. Chem. 18 (2010) 7392–7401.

[37] Pinard, M. A., Mahon, B., McKenna, R., 2015. Probing the Surface of Human Carbonic Anhydrase for Clues towards the Design of Isoform Specific Inhibitors. BioMed. Res. Int. ID453543.

[38] S. Kalinin, S. Kopylov, T. Tuccinardi, A. Sapegin, D. Dar'in, A. Angeli, C. T. Supuran, M. Krasavin, Lucky Switcheroo: Dramatic Potency and Selectivity Improvement of Imidazoline Inhibitors of Human Carbonic Anhydrase VII, ACS Med. Chem. Lett. 8 (2017) 1105-1109.

[39] M. Krasavin, M. Korsakov, M. Dorogov, T. Tuccinardi, N. Dedeoglu, C.T. Supuran, Probing the ‘bipolar nature of the carbonic anhydrase active site: Aromatic sulfonamides containing 1,3-oxazol-5-yl moiety as picomolar inhibitors of cytosolic CA I and CA II isoforms, Eur. J. Med. Chem. 101 (2015) 334-347.

[40] M. Krasavin, M. Korsakov, O. Ronzhina, T. Tuccinardi, S. Kalinin, M. Tanç, C. T. Supuran, Primary mono- and bis-sulfonamides obtained via regiospecific sulfochlorination of N-arylpyrazoles: inhibition profile against a panel of human carbonic anhydrases, J. Enz. Inhib. Med. Chem. 32 (2017) 920-934.

[41] M. Krasavin, A. Shetnev, T. Sharonova, S. Baykov, T. Tuccinardi, K. Kalinin, A. Angeli, C. T. Supuran, Heterocyclic Periphery in the Design of Carbonic Anhydrase Inhibitors: 1,2,4-Oxadiazol-5-yl Benzenesulfonamides as Potent and Selective Inhibitors of Cytosolic hCA II and Membrane-Bound hCA IX Isoforms, Bioorg. Chem. 76 (2018) 88-97.

[42] P. Koutnik, E. G. Shcherbakova, S. Gozem, M. G. Caglayan, T. Minami, P. Anzenbacher, Fluorescence-Based Assay for Carbonic Anhydrase Inhibitors, Chem 2 (2017) 272-282.

[43] Sangkaew, A., Krungkrai, J., Yompakdee, C., 2018. Development of a high throughput yeast-based screening assay for human carbonic anhydrase isozyme II inhibitors. AMB Express. 8, Article number: 124.

[44] R.G. Khalifah, The carbon dioxide hydration activity of carbonic anhydrase I. Stop-flow kinetic studies on the native human isoenzymes B and C, J. Biol. Chem. 246 (1971) 2561-2573.

[45] A. Dömling, W. Wang, K. Wang, Chemistry and Biology Of Multicomponent Reactions, Chem. Rev. 112 (2010) 3083-3135.

[46] S. Kalinin, C.T. Supuran, M. Krasavin, Multicomponent chemistry in the synthesis of carbonic anhydrase inhibitors, J. Enzyme Inhib. Med. Chem. 31 (2016), 185–199.

[47] N. Castagnoli, Jr. and M. Cushman, Condensation of succinic anhydrides with Schiff bases. Scope and mechanism, J. Org. Chem. 36 (1971) 3404–3406.

[48] M. Krasavin, M.A. Gureyev, D. Dar'in, O. Bakulina, M. Chizhova, A. Lepikhina, D. Novikova, T. Grigoreva, G. Ivanov, A. Zhumagalieva, A.V. Garabadzhiu, V. G. Tribulovich, Design, in silico prioritization and biological profiling of apoptosis-inducing lactams amenable by the Castagnoli-Cushman reaction, Bioorg. Med. Chem. 26 (2018) 2651-2673.

[49] D. Dar'in, O. Bakulina, S. Nikolskaya, I. Gluzdikov, M. Krasavin, The rare cis-configured trisubstitututed lactam products obtained by the Castagnoli-Cushman reaction in N,N-dimethylformamide, RSC Advances 6 (2016) 49411-49415

[50] A. Lepikhina, O. Bakulina, D. Dar'in, M. Krasavin, The first solvent-free synthesis of privileged γ- and δ-lactams via the Castagnoli-Cushman reaction, RSC Advances 6 (2016) 83808 – 83813.

[51] T. Tawaraishi, Preparation of N-benzoyl-4-sulfamoylbenzenesulfonamide derivatives as inhibitors of long chain fatty acid family 6 elongase, PCT Int. Appl. WO 2011102514; Chem. Abstr. 155 (2011) 328189.

[52] S. Genhenden, U. Ryde, The MM/PBSA and MM/GBSA methods to estimate ligand-binding affinities, Expert Opin. Drug Discov. 10 (2015) 449-461.

[53] M. Ferraroni, L. Luccarini, E. Masini, M. Korsakov, A. Scozzafava, C.T. Supuran, M. Krasavin, 1,3-Oxazole-based selective picomolar inhibitors of cytosolic human carbonic anhydrase II alleviate ocular hypertension in rabbits: potency is supported by X-ray crystallography of two leads, Bioorg. Med. Chem. 25 (2017) 4560-4565.

[54] Nordfors, K.M., Haapasalo, J.A., Korja, M., Niemelä, A.M., Laine, J.O., Parkkila, A., Pastoreková, S., Pastorek, J., Waheed, A.R., Sly, W.S., Parkkila, S., & Haapasalo, H.K., 2009. The tumour-associated carbonic anhydrases CA II, CA IX and CA XII in a group of medulloblastomas and supratentorial primitive neuroectodermal tumours: An association of CA IX with poor prognosis, BMC Cancer. 10, 148.

[55] Mboge, M.Y., Mahon, B.P., McKenna, R., Frost, S.C., 2018. Carbonic Anhydrases: Role in pH Control and Cancer. Metabolites. 8, 19.

[56] Uhlen, M., Zhang, C., Lee, S., Sjöstedt, E., Fagerberg, L., Bidkhori, G., Benfeitas, R., Arif, M., Liu, Z., Edfors, F., Sanli K., von Feilitzen, K., Oksvold, P., Lundberg, E., Hober, S., Nilsson, P., Mattsson, J., Schwenk, J.M., Brunnström, H., Glimelius, B., Sjöblom, T., Edqvist, P.H., Djureinovic, D., Micke, P., Lindskog, C., Mardinoglu, A., Ponten, F., 2017. A pathology atlas of the human cancer transcriptome. Science. 357 (6352), eaan2507.

[57] E. Cerami, J. Gao, U. Dogrusoz, B.E. Gross, S.O. Sumer, B.A. Aksoy, A. Jacobsen, C.J. Byrne, M.L. Heuer, E. Larsson, Antipin Y., Reva B., Goldberg A.P., Sander C., Schultz N., The cBio Cancer Genomics Portal: An open platform for exploring multidimensional cancer genomics data, Cancer Discov. 2 (2012) 401–404.

[58] Gao, J., Aksoy, B.A., Dogrusoz, U., Dresdner, G., Gross, B., Sumer, S.O., Sun, Y., Jacobsen, A., Sinha, R., Larsson, E., Cerami E., Sander C., Schultz N., 2013. Integrative Analysis of Complex Cancer Genomics and Clinical Profiles Using the cBioPortal. Sci. Signal. 6 (269), pl1

[59] Mboge, M.Y., Chen, Z., Wolff, A., Mathias, J.V., Tu, C., Brown, K.D., Bozdag, M., Carta, F., Supuran, C.T., McKenna, R., Frost, S.C., 2018. Selective inhibition of carbonic anhydrase IX over carbonic anhydrase XII in breast cancer cells using benzene sulfonamides: Disconnect between activity and growth inhibition. PLoS ONE. 13(11), e0207417.

[60] G. H. Stein, T98G: An anchorage-independent human tumor cell line that exhibits stationary phase G1 arrest in vitro, J. Cell. Physiol. 99 (1979) 43-54.

[61] K. C. Dunn, A. E. Aotaki-Keen, F. R. Putkey, L. M. Hjelmeland, ARPE-19, a human retinal pigment epithelial cell line with differentiated properties, Exp. Eye Res. 62 (1996) 155-170.

[62] M. S. Al Okail, Cobalt chloride, a chemical inducer of hypoxia-inducible factor-1a in U251 human glioblastoma cell line, J. Saudi Chem. Soc. 14 (2010) 197-201.

[63] A. Maresca, F. Carta, D. Vullo, C.T. Supuran, Dithiocarbamates strongly inhibit the β-class carbonic anhydrases from Mycobacterium tuberculosis, J. Enzyme Inhib. Med. Chem. 28 (2013) 407–411.

[64] D. Ekinci, N.I. Kurbanoglu, E. Salamci, M. Senturk, C.T. Supuran, Carbonic anhydrase inhibitors: inhibition of human and bovine isoenzymes by benzenesulphonamides, cyclitols and phenolic compounds, J. Enzyme Inhib. Med. Chem. 27 (2012) 845–848.

[65] D. Ekinci, L. Karagoz, D. Ekinci, M. Senturk, C.T. Supuran, Carbonic anhydrase inhibitors: in vitro inhibition of α isoforms (*h*CA I, *h*CA II, *b*CA III, *h*CA IV) by flavonoids, J. Enzyme Inhib. Med. Chem. 28 (2013) 283–288.

[66] C. Alp, A. Maresca, N.A. Alp, M.S. Gültekin, D. Ekinci, A. Scozzafava C.T. Supuran, Secondary/tertiary benzenesulfonamides with inhibitory action against the cytosolic human carbonic anhydrase isoforms I and II, J. Enzyme Inhib. Med. Chem. 28 (2013) 294–298.